DESY 95-047

March 1995

Interplay of Hard and Soft Physics in Small x Deep Inelastic Processes

Halina Abramowicz*

School of Physics and Astronomy

Raymond and Beverly Sackler Faculty of Exact Sciences

Tel Aviv University

Leonid Frankfurt†

School of Physics and Astronomy

Raymond and Beverly Sackler Faculty of Exact Sciences

Tel Aviv University

and

Mark Strikman‡

Pennsylvania State University, University Park

February 1, 2008

*Supported by GIF project No 127402207/93

†On leave of absence from the St.Petersburg Nuclear Physics Institute, Russia. Supported by BSF Grant No. 9200126

‡Also St.Petersburg Nuclear Physics Institute, Russia. Supported by DOE Contract DE-FG02-93ER40771

Abstract

Coherence phenomena, the increase with energy of coherence length and the non-universality of parton structure of the effective Pomeron are explained. New hard phenomena directly calculable in QCD such as diffractive electroproduction of states with $M^2 \ll Q^2$ and the color transparency phenomenon as well as new options to measure the light-cone wave functions of various hadrons are considered. An analogue of Bjorken scaling is predicted for the diffractive electroproduction of ρ mesons at large momentum transfers and for the production of large rapidity gap events, as observed at HERA. A phenomenological QCD evolution equation is suggested to calculate the basic characteristics of the large rapidity gap events. The increase of parton densities at small x as well as new means to disentangle experimentally soft and hard physics are considered. We discuss constraints on the increase of deep inelastic amplitudes with Q^2 derived from the inconsistency of QCD predictions for inclusive and exclusive processes and from unitarity of the S matrix for collisions of wave packets. New ways to probe QCD physics of hard processes at large longitudinal distances and to answer the long standing problems on the origin of the Pomeron are suggested. Unresolved problems and perspectives of small x physics are also outlined.

1 Introduction

The aim of this report is to outline QCD predictions for color coherence phenomena – a result of nontrivial interplay of hard and soft QCD physics specific for high energy processes. Coherence phenomena provide an important link between the well understood physics of hard processes and the physics of soft processes which at present is mostly phenomenological. The soft/hard interplay is elaborated for the exclusive deep inelastic processes $\gamma_L^* + N \to a + N$ for $M_a^2 \ll Q^2$ directly calculable in QCD. These processes provide new methods of investigating the structure of hadrons and the origin of the Pomeron and allow to search for new forms of hadronic matter in heavy ion collisions (for a review and

references see [1]). The phenomenon of coherence reveals itself in high energy processes through a large probability of occurrence of diffractive processes and through their specific properties. Thus in this report we concentrate mostly on diffractive processes. To explain the role of coherence in high energy processes we will consider some properties of QCD which are difficult to reconcile with intuition based on pre-QCD ideas and on perturbative QCD (PQCD) experience with medium x processes.

Let us outline briefly the experimental results pointing to a significant role of color coherent effects.

(i) Observed fast increase of parton distributions at small x and large momentum transfer Q [2, 3], which in the case of the ZEUS measurements can be parameterized as[1]

$$F_{2p}(x,Q^2) = (1-x^2)^4 \left[0.35 + 0.017 x^{-(.35+.16\log_{10} Q^2)}\right] \ . \tag{1}$$

(ii) Large cross section measured for leptoproduction of vector mesons at CERN [4] and HERA [5] which increases with energy as

$$\sigma(\gamma^* + p \to \rho + p) \propto \sigma^2_{tot}(\gamma^* + p) \ . \tag{2}$$

The energy dependence obtained by the HERA data is much faster than that of cross sections for soft two body hadron processes like elastic pp collisions. At the same time this observation is in line with the QCD predictions for the electroproduction of vector mesons and for color transparency phenomenon which are described in sections 4-6.

(iii) Large probability of occurrence of large rapidity gap events observed at HERA in the deep inelastic regime [6, 7] – this is another evidence for the important role of soft physics in deep inelastic small x processes. HERA data [8] support the dominance of events with low transverse momenta k_t. A significant magnitude of nuclear shadowing in nucleus structure functions observed at CERN and at FNAL is yet another evidence for the important role of soft physics in the deep inelastic processes at small x (for a recent

[1]This parameterization is not applicable for $Q^2 \geq 10^4$ GeV^2 where it leads to a divergence of the momentum sum rule which is precise in QCD.

review of experimental data see [9] and for a theoretical discussion of nuclear shadowing see [10, 11] and references therein).
(iv) Presence of significant fluctuations in the strength of high–energy hadron–nucleon interactions as indicated by the analysis of soft diffractive processes with protons and nuclei. In particular, the observed cross sections for inelastic diffractive production of states X off nuclei [12], $h + A \to X + A$, increases with the atomic number A significantly faster than the expected $A^{\frac{1}{3}}$ if hadrons were to interact with a nucleus as with a black body.

2 Glossary and notation.

In the course of the presentation we will use a customary notation for variables used in describing deep inelastic phenomena. For convenience we define them below:
– q denotes the 4–momentum vector of a virtual photon

$$q = (q_0, \vec{q})$$

and

$$Q^2 = -q^2.$$

– x is the Bjorken variable

$$x = \frac{Q^2}{2pq} \ ,$$

where p denotes the 4–momentum vector of the target. In the case of nuclear targets with atomic number A, x is defined as

$$x = \frac{A\ Q^2}{2pq} \ .$$

– m_N stands for the mass of the nucleon.
– s denotes the square of the center of mass energy available in the collision of a projectile with a target.

For the sake of simplicity we do not always explain all the variables if the notation is self explanatory. Thus we use E to denote the energy of a state or a particle, M for

the mass of a state and m for the mass of a particle. The subscripts explain further the objects considered.

We will try to consistently denote by N a nucleon target, by A a nuclear target and by T any target (N or A).

In the splitting of the photon into a $q\bar{q}$ we will denote by z the fraction of the photon momentum carried by one of the quarks of the pair and by k_t their transverse momentum relative to the photon direction.

When we refer to the small or low x region we have in mind x typically less than 10^{-2} which corresponds roughly to the value of x where one starts observing a rise of parton densities in the proton. Medium x refers to $10^{-2} < x < 10^{-1}$.

3 Increase of coherence length with energy.

The starting point of our discussion is the pre-QCD suggestion [13] that distances along a projectile momentum direction, l_c, which contribute to high energy processes increase with energy. The underlying nontrivial physical picture is that a sufficiently energetic projectile transforms into a hadronic component at longitudinal distances l_c from the target which are large and increase with energy. In the case of deep inelastic processes the typical longitudinal distances, in the target rest frame, are described at small x by formula [14]

$$l_c = \frac{1}{2m_N x} \ . \tag{3}$$

This formula can be also understood as a consequence of the uncertainty principle and the renormalizability of QCD. The life time τ of a virtual photon with momentum q in a hadron configuration $|n\rangle$ with mass M_n is given by the uncertainty principle as

$$\tau = \frac{1}{E_n - q_o} \simeq \frac{2q}{(M_n^2 + Q^2)} \simeq \frac{1}{2m_N x} \ . \tag{4}$$

In the last step of the derivation of the above estimate, as a consequence of QCD renormalizability, the contribution of masses $M_n^2 \gg Q^2$ can been neglected and M_n^2 can been approximated by Q^2.

In PQCD calculations of small x processes the increase with energy of l_c is a direct consequence of gauge invariance and the renormalizability of PQCD. In the nonperturbative QCD regime within the parton model, equation (4) follows from fast convergence of the integrals over transverse momenta of constituents.

We now turn to diffractive production of states X with mass M_X in the reactions $a+T \to X+T$ where a is a fast projectile and T the target. For the sake of the argument we will assume that a is a photon with virtuality Q^2. The minimal momentum transferred to the target in such a process is given by

$$t_{min} = -\frac{(M_X^2+Q^2)^2}{s^2} m_T^2 \ . \tag{5}$$

where $s = (q+p_T)^2$ is the square of the center of mass energy of the $\gamma^* T$ collision. If at sufficiently large s

$$-\frac{t_{min} r_T^2}{3} \ll 1, \tag{6}$$

the state X can be produced without disturbing the target, that is without form factor suppression. Here r_T^2 is the average quadratic radius of the target. Thus with increasing s the variety of diffractive processes increases. At the same time the number of possible intermediate parton configurations in the wave function of the photon which do not destroy the coherence of the target in the interaction also increases. In the calculation of the diffractive cross section the contribution of all these intermediate states has to be summed coherently [2]. For some hard diffractive processes the sum over hadron states can be expressed through the parton distributions in the target (sections 3 and 4). The Fourier transform of the forward diffractive amplitude into coordinate space shows that the dominant contributions come from longitudinal distances concentrated around $l \sim \frac{1}{\sqrt{-t_{min}}}$. This is essentially the same result as established in equation (4).

From all the above considerations one can conclude that the mechanism of coherence is related to a large probability of coherent diffractive processes and that l_c is a measure of the coherence length.

[2]For soft hadron processes this is implemented in the Gribov Reggeon Calculus [15].

The validity of the formula given by equation (4) has been established by B.Ioffe [14] in an analysis of the Fourier transform of data on structure functions. Since the same distances are important in vacuum and non-vacuum channels [10], another evidence for the validity of equation (4) is the energy dependence and the significant value of nuclear shadowing in photoproduction and in the deep inelastic processes at large energies (for a recent review and references see [10, 11]). To be more quantitative, let's consider a simple example which will be important for further considerations in this report. In the deep inelastic processes at HERA at $x = 10^{-4}$ the value of l_c in the proton rest frame comes out to be

$$l_c = 10^3 \text{ fm} . \tag{7}$$

This is a macroscopic distance on the scale of hadronic physics. In the simplest case of a virtual photon fluctuating into a pair of almost free quarks, the pair can propagate macroscopic distances without confinement. At LHC energies in high p_t phenomena, l_c may achieve atomic sizes – 10^5 fm. The longitudinal size of the fast $q\bar{q}$ state is rather small, $\sim \frac{1}{Q}$. However, since the $q\bar{q}$ pair is not an eigenstate of the QCD Hamiltonian, radiation of quark and gluons will occur during the space-time evolution of the wave package and its longitudinal size may reach 1 fm by the time it hits the target.

Thus the space time description of small x processes in the target rest frame leads to the conclusion that the quark-gluon configuration of the fast projectile involved in the collision is build over macroscopic distances (on the scale of hadron physics). It is this property of small x physics which will lead to many coherent phenomena. In this report we will often use the target rest frame when discussing coherence effects. Since the results cannot be frame dependent, the same effects are present in the more habitual infinite momentum reference frame. The choice of frame is thus a matter of convenience. We will show that in the infinite momentum frame the same picture leads to short range correlations in rapidity space for small x partons. This will be important for the description of large rapidity gap events.

4 Interaction cross section for small size wave packet.

One of the striking QCD predictions for hard processes dominated by large longitudinal distances is that if a hadron is found in a small size configuration of partons it interacts with a target with a small cross section. This prediction which follows from the factorization theorem for hard processes in QCD is in variance with many phenomenological approaches based on pre-QCD ideas and on quark models of hadrons.

A sufficiently energetic wave packet with zero baryon and color charges localized in a small transverse volume in the impact parameter space can be described by a $q\bar{q}$ pair . This conclusion follows from asymptotic freedom in QCD which implies that the contribution of other components is suppressed by a power of the strong coupling constant α_s and/or a power of Q^2. A familiar example of such a wave packet is a highly virtual longitudinally polarized γ^* in a $q\bar{q}$ state. Within the parton model the cross section for the interaction of such a photon with a target is suppressed by a power of Q^2. But at the same time the probability for a longitudinal photon to be in a large transverse size configuration (soft physics=parton model contribution) is suppressed by a power of Q^2. These properties explain why reactions initiated by longitudinally polarized photons are best to search for new QCD phenomena.

The cross section for a high-energy interaction of a small size $q\bar{q}$ configuration off any target can be unambiguously calculated in QCD for low x processes by applying the QCD factorization theorem. In the approximation when the leading $\alpha_s \ln \frac{Q^2}{\Lambda^2_{QCD}} \ln x$ terms are accounted for [16, 17] the result is

$$\sigma(b^2) = \frac{\pi^2}{3} \left[b^2 \alpha_s(Q^2) x G_T(x, Q^2) \right]_{x=Q^2/s, Q^2 \simeq 15/b^2} \ , \tag{8}$$

where b is the transverse distance between the quark q and the antiquark $\bar{q}$ and $G_T(x, Q^2)$ is the gluon distribution in the target T calculated within this approximation. In this equation the Q^2 evolution and the small x physics are properly taken into account through the gluon distribution.

It is possible to derive similar equation in the leading $\alpha_s \ln \frac{Q^2}{\Lambda^2_{QCD}}$ approximation one

should account for all hard processes including diagrams where (anti)quarks in the box diagram exchange gluon. The final result has the same form as eq.(8), but with $G_N(x,Q^2)$ calculated in the leading $\alpha_s \ln \frac{Q^2}{\Lambda^2_{QCD}}$ approximation. It also contains a small contribution due to sea quarks. Eq.(8) accounts for the contribution of quarks Q whose masses satisfy the condition: $l_c = \frac{2q_0}{4m_Q^2} \gg r_N$ The estimate $Q^2 \approx \frac{15}{b^2}$ was obtained in [18] by numerical analysis of the b-space representation of the cross section of the longitudinally polarized photon, σ_L, and requiring that G_T is conventional gluon distribution calculated in the leading $\alpha_s \ln \frac{Q^2}{\Lambda^2_{QCD}}$ approximation.

The generalization of equation (8) for interactions of small size wave packets with nonzero baryon number is straightforward but technically rather cumbersome [19].

There is a certain similarity between equation (8) and the two gluon exchange model of F. Low [20] and S. Nussinov [21], as well as the constituent quark 2 gluon exchange model of J. Gunion and D. Soper [22]. The factor b^2 which is present in the QCD expression (8) for the cross section is also present in these models. The major distinction between the results of QCD calculations and the two gluon exchange models is the presence of terms involving both the gluon and the sea quark distributions in equation (8). The latter are particularly relevant for the fast increase of the cross section at small x, for the seemingly slow decrease with Q^2 of higher twist processes and for the increase of nuclear shadowing with decreasing x. All those effects are characteristic for QCD as a gauge quantum field theory which predicts an increase of parton densities in hadrons with $\frac{1}{x}$ in contrast to quantum mechanical models of hadrons. Another salient property of QCD as a renormalizable quantum field theory is that for hard processes the cross sections have to be expressed in terms of parton distributions in a target, where partons are the bare particles of the QCD Lagrangian. This is not the case in the quantum mechanical models of hadrons used in [23, 24] where hard processes are modeled in terms of constituent quarks interacting through the exchange of gluons with non–zero mass. The attempt to reinterpret the gluon distribution in equation (8) as due to Weizsäcker-Williams gluons arising from the color field of constituent quarks [24] is in variance with the QCD evolution

equation analysis of the measured structure functions [25, 26, 27]. Such analysis points to an important role of the valence sea and gluons in the nonperturbative parton distributions of a hadronic target even at a very low normalization point [27, 28].

In QCD the inelastic cross section for the collision of a sufficiently energetic small size, colorless two gluon configuration off any target is,

$$\sigma(b^2) = \frac{3\pi^2}{4}\left[b^2\alpha_s(Q^2)xG_T(x,Q^2)\right]_{x=Q^2/s,Q^2=\lambda/b^2} \ , \tag{9}$$

where the parameter λ is likely to be similar to the one present in the case of scattering of a $q\bar{q}$ pair off a target. The difference compared to equation (8) is in the factor 9/4 which follows from the fact that gluons belong to the octet representation of the color group $SU(3)_c$ while quarks are color triplets.

5 Electroproduction of vector mesons in QCD.

One of the examples of a new kind of hard processes calculable in QCD is the coherent electroproduction of vector mesons off a target T,

$$\gamma^* + T \to V + T \ , \tag{10}$$

where V denotes any vector meson $(\rho, \omega, \phi, J/\Psi)$ or its excited states.

The idea behind the calculation of hard diffractive processes is that when l_c given by equation (4) exceeds the diameter of the target, the virtual photon transforms into a hadron component well before reaching the target and the final vector meson V is formed well past the target. The hadronic configuration of the final state is a result of a coherent superposition of all those hadronic fluctuations of the photon that satisfy equation (6). Thus, as in the more familiar leading twist deep inelastic processes, the calculation should take into account all possible hadronic intermediate states satisfying equation (6). The use of completeness over diffractively produced intermediate hadronic states allows to express the result in terms of quarks and gluons as in the case of other hard processes. The matrix element of electroproduction of a vector meson A can be written as a convolution of the

light cone wave function of the photon $\psi^{\gamma^* \to |n\rangle}$, the scattering amplitude for the hadron state $|n\rangle$, $A(nT)$, and the wave function of the vector meson ψ_V

$$A = \psi^{*\ \gamma^* \to |n\rangle} \otimes A(nT) \otimes \psi_V \ . \tag{11}$$

In the case of a longitudinally polarized photon with high Q^2 the intermediate state $|n\rangle$ is a $q\bar{q}$ pair. As was mentioned in the previous chapter, it can be demonstrated by direct calculations that the contribution of higher Fock state components and soft physics are suppressed by a factor $\frac{1}{Q^2}$ and/or powers of α_s. The proof of this result resembles the calculation of the total cross section for the deep inelastic scattering in QCD. The situation is qualitatively different in the case of a transversely polarized photon due to the singular behavior of the vertex $\gamma_T^* \to q\bar{q}$ when one of the partons carries a small fraction of the photon momentum. In this case soft and hard physics compete in a wide range of Q^2 (see discussion in sections 10 and 11).

To understand the applicability of PQCD for the process discussed above it is convenient to perform the Fourier transform of the amplitude into the impact parameter space which leads to

$$A \propto Q \int b^2 x G_T(x, b^2) K_0 \left(Qb\sqrt{z(1-z)} \right) \psi_V(z, b) d^2b z(1-z) dz \ , \tag{12}$$

where z denotes the fraction of the photon momentum carried by one of the quarks. Here

$$\psi^{\gamma_L^*} \propto z(1-z) Q K_0 \left(Qb\sqrt{z(1-z)} \right) \ , \tag{13}$$

where K_0 is the Hankel function of an imaginary argument. To estimate which values of b dominate in the integral we approximate $\psi_V(z, k_t)$ by $\frac{z(1-z)}{(k_t^2+\mu^2)^2}$ which corresponds to $\psi_V(z, b) \propto z(1-z) b K_1(\mu b)$. We vary $\langle k_t^2 \rangle^{1/2} = \frac{\mu}{\sqrt{2}}$ between 300 and 600 MeV/c.

We find that in case of σ_L the average transverse size $\langle b \rangle \simeq 0.25$ fm for $Q^2 = 10$ GeV$^2, x \sim 10^{-3}$ and decreases at larger Q^2 approximately as $0.3 fm \frac{3GeV}{Q}$. It also weakly decreases with decreasing x. The increase of $G_T(x, b^2)$, in equation (12) with decreasing b substantially contributes to the decrease of $\langle b \rangle$. In the case of a transversely polarized

γ^* the contribution of large b is not suppressed since

$$\psi^{\gamma_T^*} \propto \frac{\partial}{\partial b_\mu} K_0 \left(Qb\sqrt{z(1-z)} \right) \ . \tag{14}$$

and therefore the contribution of the kinematical region $z \to 0$ and $z \to 1$ where nonperturbative QCD dominates is not suppressed.

It is worth noting that $\langle b \rangle$ contributing in the calculation of σ_L – $\langle b(Q^2 = 10 \text{ GeV}^2) \rangle_{\sigma_L} \simeq 0.25$ fm is similar to that in the electroproduction of vector mesons $\langle b\,(Q^2 = 10 \text{ GeV}^2) \rangle_{\gamma_L^* \to \rho} \simeq 0.35$ fm. However for larger Q^2 the difference between the two values increases and reaches a factor of 2 for $Q^2 \sim 100$ GeV^2.

It can be shown that under certain kinematical conditions the interaction of a $q\bar{q}$ pair with the target is given by equation (8). In the leading order in $\alpha_s \ln x \ln \frac{Q^2}{\Lambda^2_{QCD}}$ the leading Feynman diagrams for the process under consideration are a hard quark box diagram with two gluons attached to it and convoluted with the amplitude for the gluon scattering off a target (see figure 1).

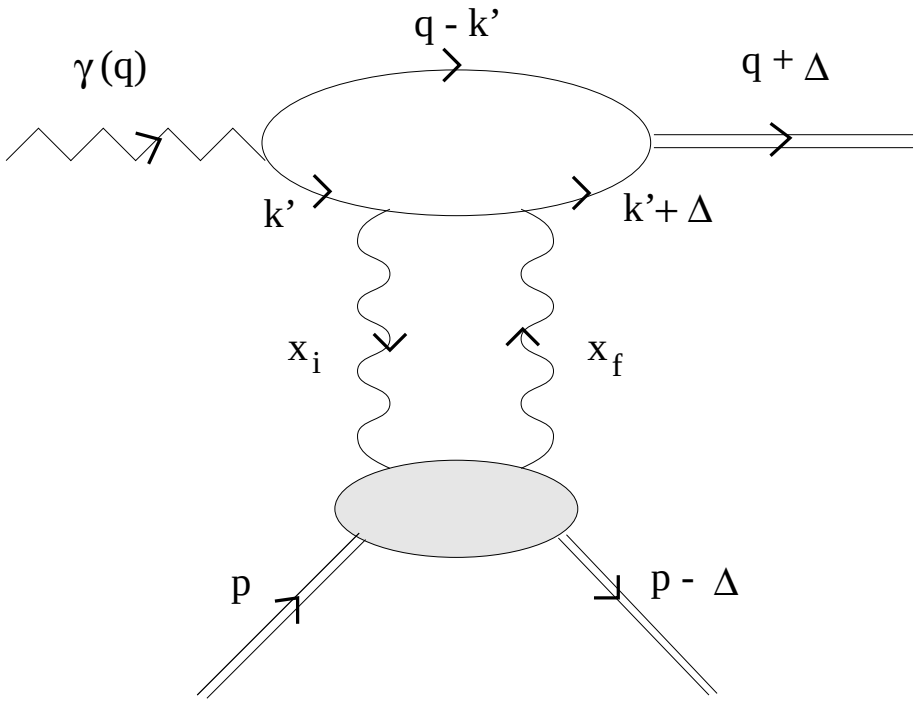

Figure 1: A typical two-gluon exchange contribution to the amplitude $\gamma^* p \to Vp$.

One can consider the same process in the leading $\alpha_s \ln \frac{Q^2}{\Lambda^2_{QCD}}$ approximation. In this case one has to include also the diagrams where one hard quark line is substituted by the gluon line. This leads to an extra term $\propto S_T(x, Q^2)$ in equation (8) and allows to treat the parton distributions in equation (8) with $\alpha_s \ln \frac{Q^2}{\Lambda^2_{QCD}}$ accuracy which is more precise than the original leading $\alpha_s \ln x \ln \frac{Q^2}{\Lambda^2_{QCD}}$ approximation in equation (8).

Since Feynman diagrams are Lorentz invariant it is possible to calculate the box part of the diagram in terms of the light-cone wave functions of the vector meson and the photon and to calculate the bottom part of the diagram in terms of the parton wave function of the proton. This mixed representation is different from the QCD improved parton model which only uses the light-cone wave function of the target.

The next step is to express this amplitude through the parton distributions in the target. In the c.m. reference frame of the *ep* system the target proton has large momentum P, while the photon four-momentum is $\left(\frac{\nu - Q^2}{4P}, \frac{-\nu - Q^2}{4P}, q_t\right)$. The longitudinal momentum

transferred to the proton in this reference frame, δ, is given by

$$\frac{\delta}{P} \approx \frac{M_V^2 + Q^2}{\nu}$$

. So the calculation of the imaginary part of the Feynman diagram of figure 1 shows that the fractions of the target momentum carried by the exchanged gluons x_i and x_f are not equal,

$$x_i - x_f = x, \quad for \quad M_V^2 \ll 1. \tag{15}$$

We neglect terms $\mathcal{O}(\frac{l_t^2}{Q^2})$ as compared to 1, with l_t the transverse momentum of the exchanged gluons. Within the QCD leading logarithmic approximation

$$\alpha_s \ln \frac{1}{x} \sim 1 \tag{16}$$

when terms $\sim \alpha_s$ are neglected, the difference between x_i and x_f can be neglected and the amplitude of the $q\bar{q}$ interaction with a target is given by equation (8) [16, 17, 29].

We are now able to calculate the cross section for the production of longitudinally polarized vector meson states when the momentum transferred to the target t tends to zero [29], but $Q^2 \to \infty$ [3]

$$\left.\frac{d\sigma^L_{\gamma^* N \to VN}}{dt}\right|_{t=0} = \frac{12\pi^2 \Gamma_{V\to e^+e^-} m_V \alpha_s^2(Q) \eta_V^2 \; I_V(Q^2)^2 |(xG_T(x,Q^2) + i\frac{\pi}{2}\frac{d}{d\ln x} xG_T(x,Q)|^2}{\alpha_{EM} Q^6 N_c^2} \; . \tag{17}$$

$\Gamma_{V\to e^+e^-}$ is the decay width of the vector meson into e^+e^-. The parameter η_V is defined as

$$\eta_V \equiv \frac{1}{2} \frac{\int \frac{dz}{z(1-z)} \Phi_V(z)}{\int dz \Phi_V(z)} \; , \tag{18}$$

where Φ_V is the light cone wave function of the vector meson. At large Q^2 equation (17) predicts a Q^2 dependence of the cross section which is substantially slower than $1/Q^6$ because the gluon densities at small x fastly increase with Q^2. Numerically, the factor

[3] In the paper of Brodsky et at [29] the factor 4 in eq.(17) has been missed. We are indebted to Z. Chan and A. Muller for pointing this out.

$\alpha_s^2(Q^2)G^2(x,Q^2)$ in equation (17) is $\propto Q^n$ with $n \sim 1$ (see figure 4). An additional Q^2 dependence of the cross section arises from the transverse momentum overlapping intergral between the light-cone wave function of the γ_L^* and that of the vector meson [18], expressed through the ratio $I_V(Q^2)$

$$I_V(Q^2) = \frac{\int_0^1 \frac{dz}{z(1-z)} \int_0^{Q^2} d^2k_t \frac{Q^4}{\left[Q^2+\frac{k_t^2+m^2}{z(1-z)}\right]^2} \psi_V(z,k_t)}{\int_0^1 \frac{dz}{z(1-z)} \int_0^{Q^2} d^2k_t \psi_V(z,k_t)}. \tag{19}$$

In ref. [29] it was assumed that $I_V(Q^2) = 1$ as for $Q^2 \to \infty$ the ratio $I_V(Q^2)$ tends to 1. But for moderate Q^2 this factor is significantly smaller than 1. For illustration we estimated $I_V(Q^2)$ for the following vector meson wave function: $\psi_V^{(1)}(z,k_t^2) = \frac{cz(1-z)}{(k_t^2+\mu^2)^2}$. The momentum dependence of this wave function corresponds to a soft dependence on the impact parameter b - $exp(-\mu b)$ in coordinate space. We choose the parameter μ so that $\langle k_t^2 \rangle^{1/2} \in 0.3 \div 0.6\ GeV/c$.

Our numerical studies show that the inclusion of the quark transverse momenta leads to several effects:

- Different k_T dependence of ψ_V leads to somewhat different Q^2 dependence of $I_V(Q^2)$. Thus electroproduction of vector mesons may become an effective way of probing k_t-dependence of the light-cone $q\bar{q}$ wave function of vector mesons.

- The Q^2 dependence of I_V for production of vector mesons build of light quarks u, d, s should be very similar.

- For electroproduction of charmonium states where $\mu_c \sim \mu \frac{m_{J\Psi}}{m_\rho}$ the asymptotic formula should be only valid for extremely large Q^2.

The NMC data [4] and the HERA data [5] on diffractive electroproduction of ρ mesons are consistent with several predictions of equation (17):

- a fast increase with energy of the cross section for electroproduction of vector mesons as seen in figure 2 from ref.[18] (proportional to $x^{-0.8}$ for $Q^2 = 10$ GeV^2) [4];

[4] This fast increase with decreasing x is absent in the non–perturbative two–gluon exchange model of

- the dominance of the longitudinal polarization $\frac{\sigma_L}{\sigma_T} \propto Q^2$;
- the absolute magnitude of the cross section within the uncertainties of the gluon densities and of the k_t dependence of the wave functions (figure 2)
- the Q^2 dependence of the cross section for $Q^2 \sim 10$ GeV^2 which can be parameterized as Q^{-n} with $n \sim 4$. The difference of n from the asymptotic value of 6 is due to the Q^2 dependence of $\alpha_s^2(Q^2)G_N^2(x,Q^2)$ and of I_V^2 which are equally important in this Q^2 range.

We discussed above (see also section 8) that the perturbative regime should dominate in the production of transversely polarized vector mesons as well, though at higher Q^2. This may manifested itself in the x-dependence of the ratio $\frac{\sigma_L}{\sigma_T}$ for fixed Q^2. At intermediate $Q^2 \sim 10$ GeV^2 where hard physics already dominates in σ_L, σ_T may still be dominated by soft nonperturbative contributions. For these Q^2 the ratio should increase with decreasing $x \sim x^2G_N^2(x,Q^2)$. At sufficiently large Q^2 where hard physics dominates for both σ_L and σ_T the ratio would not depend on x.

The t dependence of the cross section is given by the square of the two gluon form factor of the nucleon $G_{2g}(t)$. Practically no t dependence should be present in the block of γ^* gluon interaction for $-t \ll Q^2$. Thus **the t dependence should be universal for all hard diffractive processes**. Experimentally the data on diffractive production of ρ mesons for $Q^2 \geq 5$ GeV^2 [4], on photoproduction of J/Ψ mesons [31] and even on neutrinoproduction of D_s^* mesons [32] show a universal t behavior corresponding to

$$G_{2g}^2(t) = \exp(Bt) \quad \text{with} \quad B \approx 4 \text{ GeV}^{-2} \; . \tag{20}$$

A certain weak increase of B is expected with increasing incident energy due to the so called Gribov diffusion [33], but this effect is expected to be much smaller than for soft processes. However in the limit $Q^2 = const$ and $s \to \infty$ it is natural to expect an onset of

Donnachie and Landshoff [30] which leads to a cross section rising as $\sim x^{-0.14}$ at $t = 0$ and to a much weaker increase of the cross section integrated over t.

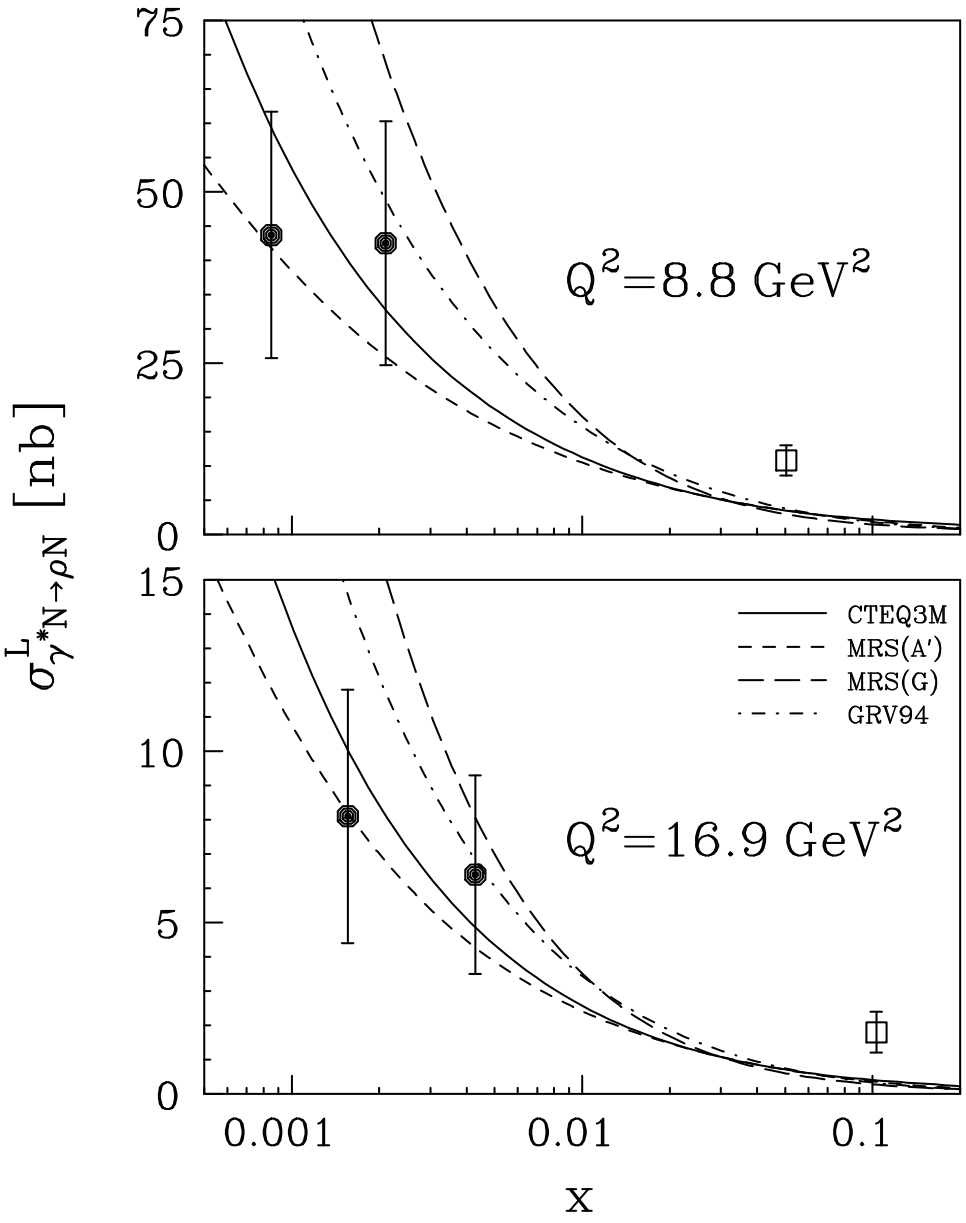

Figure 2: The total longitudinal cross section, $\sigma^L_{\gamma^* N\to\rho N}$, calculated from Eq. (17) for several recent parameterizations of the gluon density in comparison with experimental data from ZEUS [5] (full circles) and NMC [4] (squares). Typical parameters for the ρ-meson wave functions as discussed above are taken ($\langle k_t^2\rangle^{1/2} = 0.45 GeV/c$). We set $\eta_V = 3$ and parameterize the dependence of the differential cross section on the momentum transfer in exponential form with $B \approx 5$ GeV^{-2}. Note that a change of $T^2(Q^2)$ in the range corresponding to $\langle k_t^2\rangle^{1/2}$ between 0.3 GeV/c and 0.6 GeV/c introduces an extra

a soft regime, which is characterized both by a slowing down of the increase of the cross section with increasing s and by a faster increase of the slope B with s,

$$\frac{\partial \ln B}{\partial \ln s}_{|s\to\infty,Q^2=const} \approx \alpha'_{soft} \approx 0.25 GeV^{-2}. \tag{21}$$

For further discussion see section 15.

We want to point out that for $M_X^2 \ll Q^2$, the effect of QCD radiation is small. This is because bremsstrahlung corrections due to radiation of hard quarks and gluons are controlled by the parameter $\alpha_s \ln \frac{x_i}{x_f}$ which is small since in the reaction considered here $x_i \sim x_f$. This argument can be put on a formal ground within the double logarithmic approximation when only terms $\sim \alpha_s \ln \frac{1}{x} \ln \frac{Q^2}{\lambda^2}$ are taken into account. One can consider a more traditional approximation where terms $\simeq \alpha_s \ln \frac{Q^2}{\Lambda^2_{QCD}}$ are taken into account but terms $\simeq \alpha_s$ are neglected.

Within these approximations it is legitimate to neglect the contribution of the longitudinal momentum as compared to the transverse one. This is a special property of small x physics. Thus the difference between x_i and x_f leads to an insignificant correction.

Formula (17) correctly accounts for nonperturbative physics and for the diffusion to large transverse distances characteristic for Feynman diagrams, because in contrast to the naive applications of the BFKL Pomeron the diffusion of small size configurations to large transverse size is not neglected.

Electroproduction of J/Ψ mesons has been considered also in [35] within the nonrelativistic constituent quark model for J/Ψ-meson wave function in the whole Q^2 range. In the limit where we can justify the application of PQCD (eq. (17)) ($m^2_{J/\Psi} \ll Q^2$) the result of ref. [35] coincides with the nonrelativistic limit of our result if I_V is assumed to be equal 1. At the same time the inclusion of the transverse momentum distribution of c quarks in the J/Ψ wave function significantly suppresses the cross section of the diffractive electroproduction of J/Ψ mesons for $Q^2 \leq m^2_{J/\Psi}$. In particular, in the case of photoproduction calculations in the model of ref.[35] which take into account the Fermi motion of quarks using realistic charmonium models lead to a cross section smaller than the original result by a factor $4 \div 8$ depending on the model (see discussion in ref.[18]). Remember that

transverse distances essential in the photoproduction of the J/Ψ meson are $\sim \frac{3}{m_c}$ which is comparable to the average interquark distance in the J/Ψ wave function. Since the energy dependence of diffractive photoproduction of J/Ψ is consistent with pQCD prediction of [35] the disagreement with the absolute prediction may indicate an important role for the interaction with interquark potential.

It is worthwhile to notice the possibility of investigating the distribution of color in vector meson production in $\gamma^*\gamma$ collisions in reactions like $\gamma^*\gamma \to V_1 + V_2$ where V_1 is produced along γ^* and V_2 along the quasi–real photon. Study of this reaction and use of equation (17) would allow to measure the gluon density at small x in various vector mesons. It would be revealing to see how large is the difference between say $G_\rho(x,Q^2)$ and $G_\phi(x,Q^2)$, $G_{J/\Psi}(x,Q^2)$ and to investigate its dependence on the difference in radii of these vector mesons.

Another interesting process which can be calculated using the technique discussed above is the production of vector mesons in the process $\gamma_L^* + p \to V + X$ in the triple Reggeon limit when $-t \geq$ few GeV^2 and $-t \ll Q^2$. In this kinematical domain the dominant contribution is due to the scattering of the two gluons off a parton of the target $g + g +$ parton $\to$ parton. To avoid the uncertainties related to the vector meson wave function it is convenient to normalize the cross section of this process to that of the exclusive vector meson production at $t = 0$ [36]

$$\frac{\frac{d\sigma^{\gamma_L^*+p\to V+X}}{dt}}{\left.\frac{d\sigma^{\gamma_L^*+p\to V+p}}{dt}\right|_{t=0}} = \frac{9}{8\pi}\alpha_S^2\left|\ln\frac{Q^2}{k^2}\right|^2 \frac{\int_y^1 \left[G_p(y',k^2) + \frac{32}{81}S_p(y',k^2)\right]dy'}{\left[xG_p(x,Q^2)\right]^2}\,, \tag{22}$$

where S_p is the density of charged partons in the proton, $\nu = 2m_N q_o$, $x = Q^2/\nu$, $k^2 = -t$, $y = -t/2(q_o - p_{Vo})m_N$ with p_{Vo} the energy of the vector meson and all variables are defined in the nucleon rest frame.

It follows from equation (22) that the cross section of the process $\gamma_L^* + p \to V + X$ should decrease very weakly with t and therefore it is expected to be relatively large

at $-t \sim$ few GeV^2. Similarly to the approach taken in [37, 38] one can easily improve equation 22 to account for leading $\alpha_s \ln x$ terms.

Equation (22) is a particular case of the suggestion (and of the formulae) presented in reference [37], that semi–exclusive large t diffractive dissociation of a projectile accompanied by target fragmentation can be expressed through the parton distributions of the target. The advantage of the process considered here as compared to the general case is the possibility to prove the dominance of hard PQCD physics for a longitudinally polarized photon as projectile and the lack of t dependence in the vertex $\gamma^* + g \to g + V$. These advantages allow to calculate the cross section without free parameters.

Production of transversely polarized vector mesons by real or virtual photons in the double diffractive process $\gamma_T + p \to V + X$ has been calculated recently within the approximation of the BFKL Pomeron in [39]. The calculation was performed in the triple Reggeon limit for large t but $s \gg -t$. Contrary to reactions initiated by longitudinally polarized photons this calculation is model dependent; the end point nonperturbative contribution to the vertex $\gamma_T^* + g \to g + V$, and therefore to the whole amplitude, leads to a contribution which is not under theoretical control. This problem is familiar to the theoretical discussions of high Q^2 behavior of electromagnetic form factors of hadrons.

6 Properties of the electroweak production of vector mesons.

Longitudinal vector meson production is dominated by small inter-quark distances in the vector meson wave function. Therefore the factorization theorem can be used to calculate the cross section for hard diffractive processes in QCD without model assumptions. For $M_V^2 \ll Q^2$ all dependence on the quark masses and thus on flavor is only contained in the light cone wave functions of vector mesons and not in the scattering amplitudes. This prediction is non trivial since experimentally the coherent photoproduction of mesons containing strange or charm quarks is strongly suppressed as compared to the SU(4)

prediction for the ratio of the production cross section for various vector mesons, which is

$$\rho^o : \omega : \phi : J/\Psi = 9 : 1 : 2 : 8 \ . \tag{23}$$

Experimentally the suppression factor is ≈ 4 for ϕ-meson and ≈ 25 for J/Ψ. Thus QCD predicts a dramatic increase of the ϕ/ρ^o and $J/\Psi/\rho^o$ ratios at large Q^2.

Moreover, the experience with constituent quark models suggests an additional enhancement of heavier flavor production since for the heavy quarkonium states the probability for q and $\bar{q}$ to come close together is larger. In fact equation (17) derived in QCD predicts for the ratio of production of mesons V_1 and V_2 at large Q^2 that

$$\left.\frac{\sigma(\gamma_L^* + T \to V_1 + T)}{\sigma(\gamma_L^* + T \to V_2 + T)}\right|_{Q^2 \gg M_{V_1}^2, M_{V_2}^2} = \frac{M_{V_1}\Gamma_{V_1 \to e^+e^-}\eta_{V_1}^2(Q^2)}{M_{V_2}\Gamma_{V_2 \to e^+e^-}\eta_{V_2}^2(Q^2)} \ . \tag{24}$$

Based on the measured values of $\Gamma_{V \to e^+e^-}$ and estimates of η_V from QCD sum rules [40] we observe that equation (24) predicts a significant enhancement of the ϕ and J/Ψ production

$$\rho^o : \omega : \phi : J/\Psi = 9 : 1 : (2 * 1.0) : (8 * 1.5) \tag{25}$$

as compared to the SU(4) prediction. This prediction is valid for $Q^2 \gg m_V^2$ only. Pre–asymptotic effects are important in the large Q^2 range. They significantly suppress the cross section for production of charmonium states (see above discussion). Thus the value of the $J/\Psi/\rho$ ratio would be significantly below the value given by eq.(25) up to very large Q^2. For example the suppression factor is $\sim 1/2$ for $Q^2 \sim 100 GeV^2$ [18]. At the same time it is likely to change very little the predictions for ρ, ω, ϕ-meson production, since the masses of these hadrons are quite close and their $q\bar{q}$ components should be very similar.

At very large Q^2 the $q\bar{q}$ wave functions of all mesons converge to a universal asymptotic wave function with $\eta_V = 3$. In this limit further enhancement of the heavy resonance production is expected

$$\rho^o : \omega : \phi : J/\Psi = 9 : 1 : (2 * 1.2) : (8 * 3.4) \ . \tag{26}$$

It is important to investigate these ratios separately for the production of longitudinally

polarized vector mesons where hard physics dominates and for transversely polarized vector mesons where the interplay of soft and hard physics is more important.

Equation (17) is applicable also for the production of excited vector meson states with masses m_V satisfying the condition that $m_V^2 \ll Q^2$. In this limit it predicts comparable production of excited and ground states. There are no estimates of η_V for these states but it is generally believed that for ρ', ω' and ϕ' it is close to the asymptotic value, and as a rough estimate, we will assume that $\eta_V = \eta_{V'}$. Using the information on the decay widths from the Review of Particle Properties [41] we find that

$$\begin{aligned} \rho(1450) : \rho^o &\approx 0.3 \\ \omega(1420) : \omega &\approx 0.3 \\ \rho(1700) : \rho^o &\approx 1.0 \\ \omega(1600) : \omega &\approx 1.0 \\ \phi(1680) : \phi &\approx 0.6 \\ \Psi' : J/\Psi &\approx 0.5 \ . \end{aligned} \tag{27}$$

In view of substantial uncertainties in the experimental widths of most of the excited states and substantial uncertainties in the values of $\eta_{V'}$ and the ratio $\frac{I_{V'}}{I_V}$ these numbers can be considered as good to about a factor of 2. The case of Ψ' where Γ_V is well known is less ambiguous. In this case estimates using charmonium models indicate a significant suppression as compared to the asymptotic estimate up to $Q^2 \sim 20 GeV^2$ where this suppression is ~ 0.5 [18].

In spite of these uncertainties it is clear that a substantial production of excited resonance states is expected at large Q^2 at HERA. A measurement of these reactions may help to understand better the dynamics of the diffractive production as well as the light-cone minimal Fock state wave functions of the excited states. It would allow also to look for the second missing excited ϕ state which is likely to have a mass of about 1900 MeV to follow the pattern of the $\rho,\ \omega,\ J/\Psi$ families.

The relative yield of the excited states induced by virtual photons is expected to be

higher than for real photons since the Vector Dominance Model (VDM) and equation (17) lead to

$$\left.\frac{\sigma(\gamma+N\to V+N)}{\sigma(\gamma+N\to V'+N)}\frac{\sigma(\gamma_L^*+N\to V'+N)}{\sigma(\gamma_L^*+N\to V+N)}\right|_{Q^2\gg M_{V'}^2,M_V^2} = \\ = \frac{M_{V'}^2}{M_V^2}\frac{\eta_{V'}^2(Q^2)}{\eta_V^2(Q^2)}\frac{\sigma_{tot}^2(V'N)}{\sigma_{tot}^2(VN)} \geq \frac{M_{V'}^2}{M_V^2}\ . \qquad (28)$$

In the last step we used an empirical observation that for effective cross sections of $V'N$ and VN interactions which enter in the VDM model [5] $\frac{\sigma_{tot}(V'N)}{\sigma_{tot}(VN)} \leq 1$and that η_V and $\eta_{V'}$ are close to the asymptotic values for light mesons while for heavy quark systems the values of η_V' are close to the static quark value of $\eta_V = 2$.

Another interesting QCD effect is that the ratio of the cross section for the diffractive production of excited and ground states of vector mesons should increase with decreasing x and Q^2. This is because the energy denominator - $\frac{1}{\left(\frac{m_q^2+k_t^2}{z(1-z)}-m_{V'}^2\right)}$, relevant for the transition $V\to q\bar{q}$ (with no additional partons) should be large and positive. Thus the heavier the excited state, the larger Fermi momenta should be important. Thus the gluon distributions should enter at larger virtualities in the case of V' production.

Equation (17) is applicable also to vector meson production in weak processes. Consider for example the diffractive production of $D_s^{*\pm}=c\bar{s}$ meson in $W^\pm N$ scattering. To

[5]Note that these effective cross sections have no direct relation to the genuine interaction cross sections. For example, based on geometrical scaling one expects the interaction cross section to increase with the size of the projectile approximately as $R=\sigma_{tot}(\Psi' N)/\sigma_{tot}(J/\Psi N)\sim R_{\Psi'}^2/R_{J/\Psi}^2\sim 4$. However if one applies the equations of the VDM for the extraction of the cross sections from photoproduction of J/Ψ, Ψ' one finds $R\sim 0.7\sim M_{J/\Psi}^2/M_{\Psi'}^2$. This trend seems to reflect effects of color screening in the production of heavy quarkonium states [42, 10]. Note also that photoproduction data do not resolve $\rho(1430)$ and $\rho(1700)$. In the case of ρ' photoproduction off nuclei similar nuclear absorption effects are observed for the production of ρ and ρ', indicating $\sigma(\rho' N)\approx\sigma(\rho N)$. At the same time application of the vector dominance model for the process $\gamma\ p\to\rho' p$ leads to $\sigma(\rho' N)\approx 0.4\sigma(\rho N)$. The observed pattern indicates that production of ρ' is dominated by average quark-gluon configurations (large absorption cross section), while the probability of these transitions is suppressed since the transition $\gamma^*\to V$ emphasizes the role of small configurations.

calculate this cross section it is sufficient to substitute in equation (17) the electromagnetic coupling constant by $g\cos\theta_C$, where θ_C is the Cabibbo angle. Some enhancement of the D_s^* production is expected due to a larger value of $\eta_{D_s^*}$ originating from the asymmetry in the x distribution of the light and heavy quark in D_s^*.

To summarize, the investigation of exclusive diffractive processes appears as the most effective method to measure the minimal Fock $q\bar{q}$ component of the wave functions of vector mesons and the light-cone wave functions of any small mass hadron system having angular momentum 1. This would be very helpful in expanding methods of lattice QCD into the domain of high energy processes.

7 Color transparency phenomenon.

7.1 Coherent production of vector mesons off nuclei at small t

The QCD analysis described in section 4 confirms the conjecture of refs. [10, 43] that at large Q^2 vector mesons are produced in small transverse size configurations (at least for the longitudinally polarized photons) and hence the color transparency phenomenon (CT) is expected. In the case of coherent vector meson production off nuclear targets QCD prediction, in the form of equation (17), absorbs all the dependence on the atomic number in the gluon and sea quark distributions of the target. But it is well known that the evolution of parton distributions with Q^2 moves the effect of nuclear shadowing to smaller x. Thus at small but fixed x and sufficiently large Q^2 the cross section for hard diffractive processes is expected to fulfill the following relation:

$$\left.\frac{d\sigma^L_{\gamma^*+A\to X+A}}{dt}\right|_{t=0} = A^2 \left.\frac{d\sigma^L_{\gamma^*+N\to X+N}}{dt}\right|_{t=0} . \tag{29}$$

This is the so called color transparency phenomenon which leads to the validity of the impulse approximation – the nucleus is transparent for the projectile and there is no final state interactions. The onset of CT should occur at moderate Q^2 since gluon shadowing disappears fast with increasing Q^2 at fixed x [44]. If the size of the configuration is fixed

(at large but fixed Q^2) but the energy of the collision increases, shadowing effects should become more and more important since the gluon shadowing increases with decreasing x [10], (see figure 3). Moreover the analysis of the unitarity constraints in section 11 demonstrates that in the scattering off heavy nuclei screening effects should lead to very substantial suppression of coherent vector meson production cross section $\frac{d\sigma^L_{\gamma^*+A\to X+A}}{dt}\Big|_{t=0}$ for $x \sim 10^{-4}, Q^2 \sim$ 10GeV^2 as compared to the expectation of eq.(29). We shall explain in the next section that a similar CT behavior is expected for the production of transversely polarized vector mesons but at significantly larger Q^2 than for the longitudinally polarized vector mesons.

In contrast to the formula derived in QCD (equation (17)) the two gluon exchange constituent quark model [22] predicts no increase of the cross section at small x. Quark models and the Glauber approximation (used in particular in [45]) are in variance with the factorization theorem in QCD even if formula (8) obtained in [16, 17] is used for the nucleon target since they predict the disappearance of shadowing at fixed Q^2 when x decreases.

As explained above, the preliminary HERA data indicate that PQCD predictions contained in formula (17) are applicable already for $Q^2 \sim 10$ GeV^2. Obviously this is an implicit confirmation of the color transparency logic since it confirms both the presence of small transverse configurations in the ρ meson and the smallness of their interactions with hadrons. It would be important to investigate further these effects more directly at ultra high energies. To this end we consider briefly the scattering off the lightest nuclei [46]. Note that there are discussions to accelerate deuterons at HERA and to polarize them in order to measure the parton distributions in the neutron.

7.2 Color transparency effects in $\gamma^*_L + D(A) \to V_L + D(A)$.

The very existence of the color coherence effects leads to a rather nontrivial dependence of the cross sections of hard diffractive processes on x, Q^2. To elucidate this point we consider in this section diffractive electroproduction of vector mesons off the deuteron.

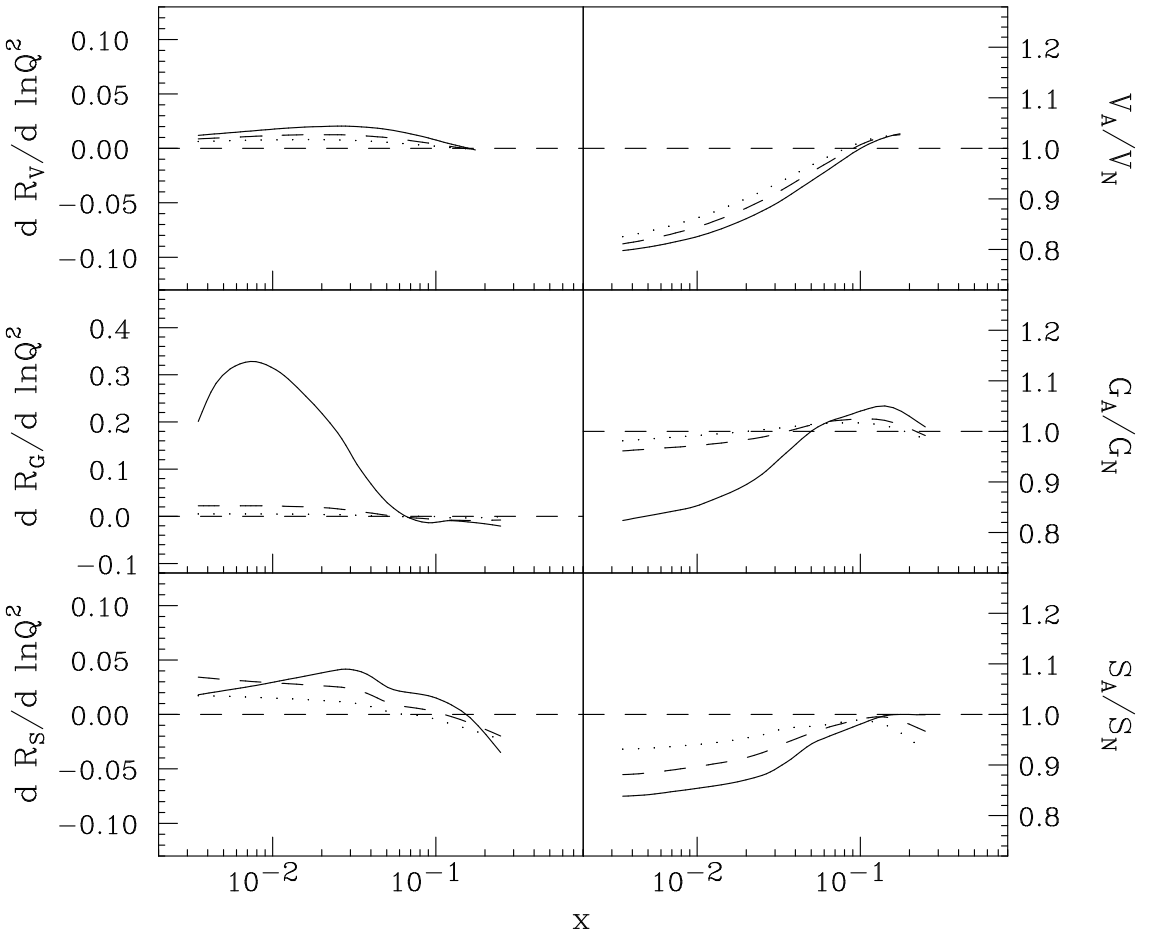

Figure 3: The ratios R_S, R_V, and R_G of sea, valence and gluon distributions for A=40 and A=2 and (left) their logarithmic derivatives, $dR_{S(V,G)}(x,Q^2)/d(\ln Q^2)$ as a function of x for $Q^2 = 4$ GeV^2 (full line), $Q^2 = 25$ GeV^2 (dashed line) and $Q^2 = 100$ GeV^2 (dotted line).

First, let us consider the leading twist effect. It follows from eq.(29) that at t=0 the amplitude of this process is proportional to the parton density in the deuteron. The nuclear effect in the leasing twist depend on x, Q^2 in a rather complicated way. At $x \sim 0.1$ and $Q^2 \sim \ \ few \ \ GeV^2$ - the kinematics of the HERMES facility the gluon density in nuclei is significantly enhanced: $\frac{G_A(x,Q^2)}{AG_N(x,Q^2)} > 1$. This effect follows from the need to reconcile the momentum and baryon sum rules with the $\frac{F_{2A}(x,Q^2)}{F_{2N}(x,Q^2)}$ data [44]. The dynamical mechanism relevant for the gluon enhancement is not understood so far. One example of the Feynman diagrams which may lead to such an enhancement is the propagation of color states in nuclei and their mixing with multinucleon states via gluon exchanges. Since the gluon exchange amplitude is real the contribution of such diagrams corresponds to enhancement of the gluon field not the shadowing. Legitimate calculations of such a mechanism are absent at present.

Consequently QCD predicts an enhancement but no shadowing for the electroproduction of vector mesons at $t = 0$ off the deuteron at $x \sim 0.1$. This effect should die out rather rapidly with increase of Q^2 due to the QCD evolution of parton distributions with Q^2 (cf. Fig. for the Q^2 dependence of parton distributions).

At sufficiently small $x \leq 10^{-2}$ shadowing of gluon distribution dominates. We will restrict the discussion to the region of sufficiently large $x \geq 10^{-4}$ where interaction of a small $q\bar{q}$ state with a nucleon, $\sigma_{q\bar{q}N}(b^2, x)$ which is given by eq.(8) is small as compared to the unitarity limit and therefore QCD evolution equations seem to be applicable. In this kinematics one expects a fast decrease of shadowing with increase of Q^2.

Obviously, at $t \approx t_{min}$ shadowing effects are small since inter-nucleon distance in the deuteron are comparatively large. To enhance these effects it would be advantageous to study experimentally the coherent electroproduction of vector mesons at $|t| \geq 0.5 GeV^2$ where an interesting diffraction pattern with secondary maximum was observed long time ago for photoproduction of ρ-meson. This pattern at $Q^2 = 0$ arises within the vector dominance model as a result of the vector meson rescatterings. At large Q^2 QCD predicts more complicated behavior.

Let us consider first the rescatterings of the produced $q\bar{q}$ pair of small size b. The scattering amplitude is given by the sum of two terms, one given by the impulse approximation and the other due to double scattering [6]

$$\frac{d\sigma_L(\gamma^* + D \to V + D)}{dt} = \frac{1}{16\pi}\Big|\int \Big[2S_D(t) f_{\gamma^* N\to VN}(x, b^2, r_t) + \int \frac{i}{8\pi^2}\, f_{\gamma_L^* N\to VN}(x, b, Q^2, r_t/2 - k_t) f_{q\bar{q},N}(x, b, r_t/2 + k_t) S_D(4k_t^2) \psi_{\gamma^*}(z, b, Q^2)\psi_V(z, b) dz d^2k_t\Big]\, d^2b\Big|^2 \ , \tag{30}$$

where $t = -r_t^2$, $S_D(t)$ is the deuteron form factor, and $f_{q\bar{q},N}(x, b, r_t/2+k_t)$ is the amplitude for the elastic rescattering of the $q\bar{q}$ pair. For simplicity we ignore here the spin indices. For the interaction of a small transverse size $q\bar{q}$ configuration small impact parameters b dominate in equation(30). Hence the CT prediction of formula (8) is that at small but fixed x with increasing Q^2 the relative contribution of the second term should be proportional to $\frac{1}{Q^2} x G_N(x, Q^2)$. Since at $-t \geq -t_0 \sim 0.5$ GeV^2 the elastic cross section is dominated by the square of the second term, this mechanism leads in this region to a cross section which is extremely sensitive to the CT effects. In particular, the ratio

$$\left.\frac{d\sigma^{\gamma_L^*+D\to V+D}}{dt}\right|_{-t\geq -t_0} \Big/ \left.\frac{d\sigma^{\gamma_L^*+D\to V+D}}{dt}\right|_{-t=0} = \left|\frac{\langle\sigma_{q\bar{q}N}(b)\rangle}{4\pi}\left\langle\frac{1}{R^2}\right\rangle\right|^2 \frac{\exp Bt}{4} \propto \frac{x^2 G_N^2(x, Q^2)\exp Bt}{Q^4}, \tag{31}$$

where

$$\langle\sigma_{q\bar{q}N}(b)\rangle = \frac{\int d^2b \psi_{\gamma_L^*}(b)\psi_V(b)\sigma^2_{q\bar{q}N}(b)}{\int d^2b \psi_{\gamma_L^*}(b)\psi_V(b)\sigma_{q\bar{q}N}(b)} \tag{32}$$

should strongly decrease with increasing Q^2 and flatten for sufficiently large Q^2 to a leading twist behavior due to the space-time evolution of the $q\bar{q}$ configurations. On the contrary at fixed Q^2 this ratio should increase with decreasing x. Here $B = B_{\gamma^* N}/2$ with $B_{\gamma^* N}$ denoting the slope of the differential cross section for the elementary $\gamma^* + N \to V + N$

[6] Since the relevant b are small we neglect here in the first approximation effects of the leading twist nuclear shadowing induced by the space-time evolution of the $q\bar{q}$ pair leading to the formation of large spatial size quark-gluon configurations.

reaction and $\left\langle \frac{1}{R^2} \right\rangle = \int d^3r r^{-2} \psi_D^2(r)$. The large t ($-t \geq 0.5$ GeV^2) dependence of the cross section in equation (31), $\frac{d\sigma}{dt} \propto \exp(B't)$ with $B' \sim 2$ GeV^{-2}, is significantly weaker than in the Glauber model where B' is expected to be

$$B' = \frac{B_{\gamma^* N} B_{\gamma N}}{B_{\gamma^* N} + B_{\gamma N}} \approx 3 \text{ GeV}^{-2} \ . \tag{33}$$

We neglected here the deuteron quadrupole form factor effects. They lead to a contribution to the cross section which does not interfere with the electric transition and for which Glauber effects are small. This contribution fills the minimum due to the interference of the impulse and double scattering terms [47]. However this contribution to the cross section can be significantly suppressed by using a polarized deuteron target. Similar effects should be present for the scattering off heavier nuclei, like $^{3,4}He$. The measurement of the depth of the Glauber minimum due to the interference of the amplitude given by the impulse approximation with rescattering amplitudes would allow to check another feature of expression (17), namely the large value of the real part of the production amplitude $Ref/Imf \sim \pi n/2 \sim 0.5$, where n characterizes the rate of increase of the gluon density at small x, $xG_N(x,Q^2) \propto x^{-n}$. In this discussion we neglected the leading twist mechanism of double rescattering related to the leading twist nuclear shadowing. It is likely to have a similar $t-$dependence as the term considered previously. It may compete with the mechanism we discussed above in a certain x, Q^2 range. This question requires further studies. In any case it is clear that in a wide kinematic range the relative height of the secondary maximum would be strongly suppressed as compared to the case of vector meson production by real photons. At very small x for Q^2 where $\sigma_{q\bar{q}N}$ is close to unitarity bound this suppression may disappear. This would establish the x, Q^2 range where color transparency should disappear.

Recent FNAL data on incoherent diffractive electroproduction of vector mesons off nuclear targets [48] did find an increase of nuclear transparency with increasing Q^2 as predicted in [10, 43, 45]. However in this experiment the increase of Q^2 is correlated with the increase of the average x and a significant effect is reported for a Q^2 range where $\langle x \rangle$ corresponds to average longitudinal distances which are comparable with the nuclear

radius $l_c = \frac{1}{2m_N x} \sim R_A$. It is well known that at large x shadowing disappears for hard processes. Thus it is necessary to investigate theoretically to what extent the observed increase of transparency is explained by the effects of finite longitudinal distances. The ideas discussed in this report do not apply directly to color transparency phenomena at moderate energies. For a recent review of this field we refer the interested reader to [1].

8 Electroproduction of photons.

The diffractive process $\gamma^* + p \to \gamma + p$ offers another interesting possibility to investigate the interplay between soft and hard physics and to measure the gluon distribution in the proton. We shall consider the forward scattering in which case only the transverse polarization of the projectile photon contributes to the cross section. This follows from helicity conservation. In this process, in contrast to reactions initiated by longitudinally polarized highly virtual photons, soft (nonperturbative) QCD physics is not suppressed. As a result, theoretical predictions are more limited. Within QCD one can calculate unambiguously only the derivative of the amplitude over $\ln \frac{Q^2}{Q_o^2}$ but not the amplitude itself. However for sufficiently small x and large Q^2, when $\alpha_s(Q_o^2) \ln \frac{Q^2}{Q_o^2} \ln x$ is large, PQCD predicts the asymptotic behavior of the whole amplitude.

It is convenient to decompose the forward scattering amplitude for the process $\gamma^* + p \to \gamma + p$ into invariant structure functions in a way similar to the case of deep inelastic electron-nucleon scattering. Introducing the invariant structure function $H(x, Q^2)$, an analogue of $F_1(x, Q^2)$ familiar from deep inelastic electron scattering off a proton, we have

$$\left.\frac{d\sigma}{dt}^{\gamma^*+N\to\gamma+N}\right|_{t=0} = \pi\alpha_{em}^2 \frac{H(x,Q^2)^2}{s^2} \ . \tag{34}$$

When Q^2 is sufficiently large, QCD allows to calculate the Q^2 evolution of the amplitude in terms of the parton distributions in the target. As in the case of deep inelastic processes it is convenient to decompose $H(x, Q^2)$ in terms of photon scattering off flavors

of type i

$$H(x,Q^2) = \sum_i e_i^2 h_i(x,Q^2) \ , \tag{35}$$

where the sum runs over the different flavors i with electric charge e_i. It is easy to deduce the differential equation for h_i, the analogue of the evolution equation for the parton distributions.

$$\frac{dh_i(x,Q^2)}{d\ln Q^2} = \frac{\alpha_s(Q^2)}{2\pi}\int\frac{dz}{z}\left[P_{qg}\left(\frac{x}{z}\right)G_p(z,Q^2)+ P_{qq}\left(\frac{x}{z}\right)q_i(z,Q^2)\right]\left[1+\frac{x}{z}\left(1-\frac{x}{z}\right)\right]+\mathcal{O}(\alpha_s^2) \ . \tag{36}$$

Here P_{qq} and P_{qg} are the splitting functions of the GLDAP evolution equation [34] . The factor $1+\frac{x}{z}\left(1-\frac{x}{z}\right)$ takes into account the difference of the virtualities of the initial and final photon. The solution of this equation is

$$h_i(x,Q^2) = h_i(x,Q_0^2) + \frac{\alpha_s(Q^2)}{2\pi}\int\limits_{\ln Q_o^2}^{\ln Q^2} d\ln Q_1^2 \int\limits_x^1 \frac{dz}{z} \left[P_{qg}\left(\frac{x}{z}\right)G_p(z,Q_1^2) + P_{qq}\left(\frac{x}{z}\right)q_i(z,Q_1^2)\right]\left[1+\frac{x}{z}\left(1-\frac{x}{z}\right)\right]+\mathcal{O}(\alpha_s^2) \ . \tag{37}$$

Usually it is assumed that the soft components of the parton distributions increase at small x more slowly than the hard ones. If this is the case, at sufficiently small x, in the leading $\alpha_s \ln x$ approximation, the first term in equation (37) can be neglected. As a result one can obtain the asymptotic formula for the whole $H(x,Q^2)$ and not only for its derivative.

Similarly to the case of electroproduction of photons it is not difficult to generalize the Q^2 evolution equation to the amplitude for the diffractive production of transversely polarized vector mesons. One of the consequences of this evolution equation is that, at asymptotically large Q^2 and small x, the production cross section has the same dependence on the atomic number of a target as in the case of longitudinally polarized vector mesons.

9 Coherent Pomeron.

It is interesting to consider high-energy hard processes in the diffractive regime with the requirement that there is a large rapidity gap between the diffractive system containing the high p_t jets and the target which can remain either in the ground state or convert to a system of hadrons. In PQCD such a process can be described as an exchange of a hard gluon accompanied by a system of extra gluons which together form a color neutral state. It was predicted [37] that such processes should occur in leading twist. (Note that in reference [61] it was stated that this process should rather be a higher twist effect. This statement was due to some specific assumptions about the properties of the triple Pomeron vertex).

The simplest example is in the triple Reggeon limit the production of high p_t jets in a process like

$$h + p \to jet_1 + jet_2 + X + p \tag{38}$$

where the final state proton carries practically the whole momentum of the initial proton. The initial particle can be any particle including a virtual photon. To probe the new PQCD hard physics the idea [37] is to select a final proton with a large transverse momentum k_t. One can demonstrate that this selection tends to compress initial and final protons in small configurations at the moment of collision. In this case the use of the PQCD two gluon exchange or two–gluon ladder diagrams becomes legitimate. A nontrivial property of these processes is a strong asymmetry between the fractions of the target momentum carried by the two gluons (the contribution of the symmetric configurations is a higher twist effect with the scale determined by the invariant mass of the produced two jets [49]). Thus one expects gluon bremsstrahlung to play a certain role [50]. However since the proton is in a configuration of a size $\sim \frac{1}{k_t}$ this radiation is suppressed by the small coupling constant: $\sim \alpha_s(k_t^2)\ln(\frac{p_t^2}{k_t^2})$. When k_t tends to 0 this radiation may suppress significantly the probability of occurrence of events with large rapidity gaps.

The prediction is that such a process appears as a leading twist effect [37]

$$\frac{d\sigma}{dp_t^2} \sim \frac{1}{p_t^4} \ . \tag{39}$$

This prediction is in an apparent contradiction with a naive application of the factorization theorem in QCD which states that the sum of the diagrams with such soft gluon exchanges cancels in the inclusive cross section. However in reaction (38) we selected a certain final state with a white nucleon hence the usual proof of the factorization theorem does not hold anymore — there is no cancelation between absorption and radiation of soft gluons [49]. This conclusion was checked in a simple QED model with scalar quarks [51].

It was suggested by Ingelman and Schlein [52] to consider scattering off the Pomeron as if the Pomeron were an ordinary particle and to define parton distributions in the effective Pomeron. In this language the mechanism of hard interaction in diffraction discussed above would contribute to the parton distribution in the Pomeron a term proportional to

$$\delta(1-x) \quad \text{or} \quad \frac{1}{(1-x)} \ . \tag{40}$$

This term corresponds to an interaction in which the Pomeron acts as a whole. Hence the term coherent Pomeron. In this kinematical configuration the two jets carry practically all the longitudinal momentum of the Pomeron. The extra gluon bremsstrahlung discussed previously renders the x dependence somewhat less singular at $x \to 1$ but the peak should be concentrated at large x [50, 49]. There are no other known mechanisms generating a peak at large x. The recent UA(8) data [53] on the reaction $p+\bar{p} \to jet_1+jet_2+X+p$, with the proton transverse momentum in the range 2 GeV$^2 \geq k_t^2 \geq 1$ GeV^2, seem to indicate that a significant fraction of the two jet events corresponds to the $x \sim 1$ kinematics. It is thus possible that the coherent Pomeron contributes significantly to the observed cross section [7].

[7] The coherent production of high p_t jets by a real photon has been first discussed by Donnachie and Landshoff [54] and then rediscussed in reference [55]. This process, discussed in the next section, gives a negligible contribution in the kinematic regime characteristic for the coherent Pomeron.

The prediction is that the contribution of the coherent Pomeron to diffractive electroproduction of dijets at $p_t^2 \gg Q^2$ should be suppressed by an additional power of Q^2

$$\frac{d\sigma^{\gamma^*+p\to 2jets+X+p}}{dp_t^2} \sim \frac{1}{p_t^4}\frac{1}{Q^2}$$

as compared to

$$\frac{d\sigma^{\gamma^*+p\to 2jets+X}}{dp_t^2} \sim \frac{1}{p_t^4}$$

for other hard processes originating from the hard structure of the virtual photon.

The complicated nature of the effective Pomeron should manifested itself in several ways in hard diffraction [37, 49].

(i) There should be a significant suppression of the coherent Pomeron mechanism at small t due to screening (absorptive) effects since at small t the nucleon interacts in an average configuration. This suppression should be larger for pp scattering than for γp scattering since absorptive corrections increase with the increase of the total cross section (for γp interaction the VDM effective total cross section at HERA energies is ≤ 30 mb).

(ii) Due to the contribution of soft physics, the effective Pomeron structure function as determined from the low t diffractive processes should be softer than for large t diffraction.

Therefore it would be very important to compare hard diffractive processes induced by different projectiles and to look for deviations from the predictions based on the simplest assumption that the Pomeron has an universal parton distribution [26].

10 Forward electroproduction of jets.

Forward diffractive photo and electroproduction of high p_t jets off a nucleon target (in the photon fragmentation region) $\gamma^* + N \to jet_1 + jet_2 + N$ is another promising process to investigate the interplay of soft and hard physics. We shall confine our discussion to the kinematical region

$$\frac{-\langle r_N^2\rangle\, t_{min}}{3} = \left(\frac{Q^2+M_{q\bar{q}}^2}{2q_0}\right)^2 \frac{\langle r_N^2\rangle}{3} \ll 1, \tag{41}$$

where

$$M_{q\bar{q}}^2 = \frac{(m_q^2 + p_t^2)}{z(1-z)} \tag{42}$$

is the square of the invariant mass of the produced $q\bar{q}$ system, m_q is the mass of quarks and z is the fraction of photon momentum carried by the q or $\bar{q}$. In this regime the coherence of the produced hadron states allows to express the amplitude through the gluon distribution in the target.

An interesting effect occurs in the photoproduction of high p_t jets. The contribution of a single Feynman diagram with the 2 gluon exchange in the t channel contains terms $R_1 \approx \frac{p_t\ \mu}{p_t^2+M^2}$ and $R_2 \approx \frac{m}{p_t^2}$. Here m is the mass of a bare quark, M can be calculated through m in pQCD but in general accounts for the nonperturbative physics. We omit constants and σ matrixes in this dimensional estimate and restrict ourselves to the contribution of large p_t only. A cancelation occurs when the sum of diagrams is considered. It accounts for the fact that the sum of diagrams describes the scattering of a colorless dipole.

Naively we should expect that after cancelation R_1 term should become $R_1 \approx \frac{p_t\ \mu}{(p_t^2+M^2)^2}$. But in reality it becomes $R_1 \approx \frac{M^2 p_t\ \mu}{(p_t^2+M^2)^3} \approx \frac{1}{p_t^5}$. R_2 term after cancelation in the sum of diagrams becomes $R_2 \approx \frac{m}{p_t^4}$. Thus cross section of forward photoproduction of $q\bar{q}$ pair $d\sigma/dtdp_t^2$ contains terms: $\frac{m^2}{p_t^8}$ [55], $\frac{M^4}{p_t^{10}}$ and $\frac{M^2 m}{p_t^9}$.

Since mass of light quark is small it is reasonable to put it 0. It is not legitimate to put $M = 0$. So expected asymptotical behavior is $\frac{M^4}{p_t^{10}}$. Thus photoproduction of charm should dominate hard diffractive photoproduction processes for $p_t \geq m_c$ [55].

Photoproduction of high p_t jets originating from the fragmentation of light flavors is predominantly due to next to leading order processes in α_s.

The diffractive electroproduction of dijets seems to be the dominant process in the region of $M_{q\bar{q}}^2 \leq Q^2$, while in the region $M_{q\bar{q}}^2 \gg Q^2$ exclusive dijet production is one of many competing processes contributing to the diffractive sector like radiation of gluons from quark and gluon lines.

In the approximation when only leading $\alpha_s \ln x$ terms are kept, the off mass shell effects in the amplitude for the $q\bar{q}$ interaction with a target are unimportant. Therefore the total

cross section of diffractive electroproduction of jets by longitudinally polarized photons can be calculated by applying the optical theorem for the elastic $q\bar{q}$ scattering off a nucleon target and equation (8) for the total cross section of $q\bar{q}$ scattering off a nucleon:

$$\sigma(\gamma_L^* + N \to jet_1 + jet_2 + N) = \frac{1}{16\pi B} \int \psi^2_{\gamma_L^*}(z,b) \cdot (\sigma(b^2))^2 dz d^2b \tag{43}$$

Here B is the slope of the two gluon form factor discussed in section 4 and $\psi_{\gamma_L^*}(z,b)$ is the wave function of the longitudinally polarized photon. Essentially the same equation is valid for the production by transversely polarized virtual photons of two jets which share equally the momentum of the projectile photon.

In [56] it has been assumed that diffractive production of jets off a proton is a hard process at each stage. The formula obtained under this assumption resembles equation (43) with leading $\alpha_s \ln \frac{Q^2}{\Lambda^2_{QCD}} \ln \frac{1}{x}$ with the PQCD part of the gluon distribution in a target. In view of the nontrivial interplay of soft and hard physics of large longitudinal distances this approach is questionable in QCD if x is not extremely small. It is most easily seen when one considers the effect of nuclear shadowing in diffractive electroproduction of jets. If the assumption that hard PQCD dominates at each stage of the interaction were correct, nuclear shadowing should be numerically small and suppressed by a power of Q^2. The discussion in section 6 indicates that, on the contrary, in QCD at sufficiently small x and fixed Q^2 nuclear shadowing is expected to be substantial and universal for all hard processes. This conclusion is supported by current data on nuclear shadowing in deep inelastic processes.

Dijet production has been also considered in the constituent quark model of the proton [23, 24]. In this approach the cross section for diffraction is expressed through a convolution of the quark distribution in the virtual photon, the distribution of constituent quarks in the proton and their interaction cross section. A later generalization of this model [24] includes the gluon field of constituent quarks. In QCD though, hard processes have to be expressed in terms of bare partons and not constituent ones. This is due to the use of completeness of the intermediate hadronic states in hard processes.

Equation (43) implies that in this higher twist effect the contribution of large b, that

is of the nonperturbative QCD, is enhanced as compared to the large b contribution to the total cross section. This result has been anticipated in the pre-QCD times [73] and has been confirmed in QCD [10]. A similar conclusion has been reached in the constituent quark model [24] approach even though it ignores the increase of parton distributions at small b characteristic for QCD (see discussion in section 11). In QCD the hard contribution is expected to become dominant only at rather small x and large Q^2. A similar conclusion has been reached for the cross section of diffractive processes, calculated in the approximation of the BFKL Pomeron [57], in the triple Reggeon region when the mass of the produced hadronic system is sufficiently large $M^2 \gg Q^2$.

Note that PQCD diagrams which were found to dominate in the large mass diffraction [57] are different from those expected from the naive application of the BFKL Pomeron [56, 24] and lead to different formulae.

To calculate this process within the more conventional leading $\alpha_s \ln Q^2$ approximation it is necessary to realize that in the kinematical region where $M^2_{q\bar{q}} \sim Q^2$ the fractions of nucleon momentum carried by the exchanged gluons are strongly different, $x_{\rm hard} \simeq 2x$ but $x_{\rm soft} \ll x$. This is qualitatively different from the case of the vector meson production considered in section 4 in which the two values of x of the gluons were comparable. This is because in the case of dijet production the masses of the intermediate states are approximately equal to the mass of the final state. As a result of the asymmetry of the two x values the overlap integral between the parton wave functions of the initial and final protons cannot be expressed directly through the gluon distribution in the target. However at sufficiently small x and large Q^2, when the parameter $\frac{\alpha_s}{\pi} \ln x \ln \frac{Q^2}{\Lambda^2} \sim 1$, electroproduction of high p_t dijets can be expressed through the gluon distribution in a target but in a more complex way. In this particular case the factorization theorem can be applied after the first two hard rungs attached to the photon line, which have to be calculated exactly. The lower part of the diagram can be then expressed through the gluon distribution in the target since the asymmetry between the gluons becomes unimportant in the softer blob.

The proof is the same as for the vector meson electroproduction [9] . The cross section is proportional to

$$\left.\frac{d\sigma^{\gamma^*+N\to jet_1+jet_2+N}}{dt}\right|_{t=0} \propto \left|A_{\gamma^*+gg\to jet_1+jet_2}\right|^2 \left|\tilde{x}G_N(\tilde{x},Q^2)\right|^2 \propto \left(\frac{\alpha_s(Q^2)xG_N(x,Q^2)}{Q^2}\right)^2, \tag{44}$$

where $\tilde{x}$ is the average x of the gluons in the $\gamma^* + gg \to jet_1 + jet_2$ amplitude, $\tilde{x} \gg x$, and $A_{\gamma^*+gg\to jet_1+jet_2}$ is the hard scattering amplitude (which includes 2 hard rungs) calculated in PQCD.

One of the nontrivial predictions of QCD is that the decomposition of the cross section for a longitudinally polarized photon in powers of Q^2 becomes inefficient at small x. This is because additional powers of $1/Q^2$ are compensated to a large extent by the increase with Q^2 of $\left[\alpha_s(Q^2)xG(x,Q^2)\right]^2 \sim \frac{Q}{x}$ (see figure 4 and equations (44), (43)). Thus the prediction of QCD is that electroproduction of hadron states with $M_X^2 \ll Q^2$ by longitudinally polarized photons, formally a higher twist effect, should in practice depend on Q^2 rather mildly. The contribution of such higher twist effects to the total cross section for diffractive processes may be considerable, as high as $30 - 40\%$. One of the observed channels, the electroproduction of ρ mesons, constitutes probably up to 10% of the total cross section for diffractive processes. So far a detailed quantitative analysis of this important issue is missing. On the experimental side, it would be extremely important to separate the longitudinal and transverse contributions to diffraction.

11 Limiting behavior of cross sections for hard processes

Both the GLDAP QCD evolution equation [34] and the BFKL equation [58] predict a significant increase of parton distributions at large Q^2 and small x. This expectation is consistent with a fast increase of parton densities with decreasing x observed at HERA.

[9] We are indebted to A.Mueller for the discussion of this problem.

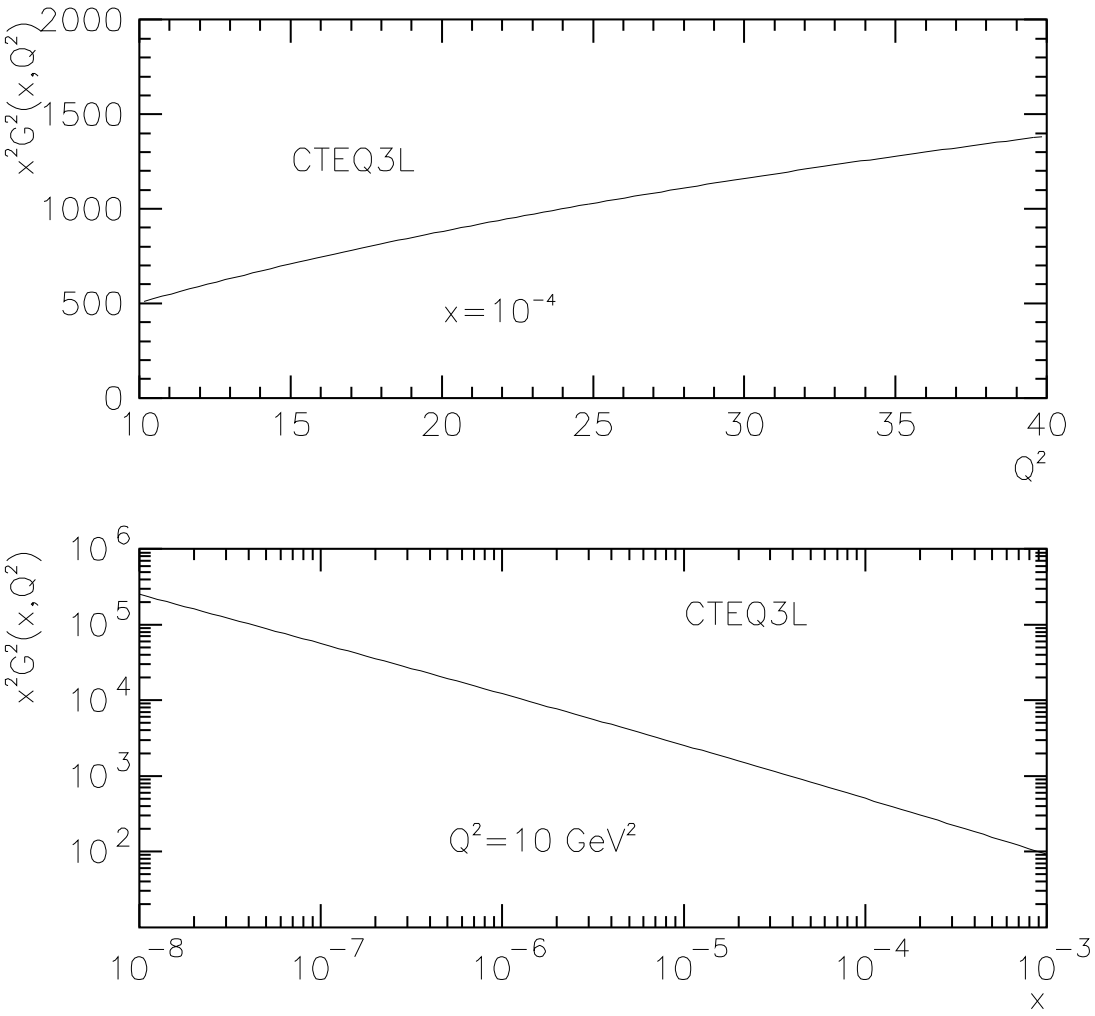

Figure 4: The square of the $xG(x, Q^2)$ distribution as a function of Q^2 for a fixed $x = 10^{-4}$ and as a function of x for a fixed $Q^2 = 10$ GeV^2 for the CTEQ3L parameterization.

The question then arises whether the increase of parton distributions with increasing Q^2 and $\frac{1}{x}$ will stop or will continue forever. The evident lack of elastic unitarity condition for the electromagnetic amplitude precludes the use of theoretical approaches which lead to Froissart limit for the on mass shell amplitude. (The elastic contribution to the unitarity condition is suppressed by power of the electromagnetic coupling constant.) At the same time it is well known that the PQCD calculation of the scattering of two body amplitude via the sum of leading logarithms runs, at sufficiently large energies, into conflict with s-channel unitarity – violation of the Froissart limit. How to restore unitarity still remains an open question. Thus the leading logarithms approximation is expected to be applicable only in a restricted kinematical region.

Our aim here is to estimate the kinematical region of applicability of the leading logarithms approximation from the requirement of self–consistency of QCD calculations of the hard diffractive processes discussed in sections 4–9. We will also consider the unitarity condition for the scattering of colorless wave packets to deduce restrictions on the limiting behavior of cross sections for deep inelastic processes. The idea is rather simple. In QCD, within the leading $\alpha_s \ln Q^2$ and/or $\alpha_s \ln x$ approximation $\sigma_L^{tot}(\gamma^* + p)$ should increase at small x like $xG_p(x, Q^2)$. At the same time the cross sections for diffractive electroproduction of states with $M_X^2 \ll Q^2$, $\sigma_L(\gamma^* + p \to X + p)$, is proportional to $[xG_p(x, Q^2)]^2$ as discussed in section 4. Thus the requirement that $\sigma_L^{tot}(\gamma^* + p) \gg \sigma_L(\gamma^* + p \to X + p)$ will lead to a restriction on the region of applicability of the leading logarithm formulae. We do not have as yet measurements of the total cross section for longitudinal virtual photons, but we can estimate in which range of x the contribution from small mass diffractive production will be comparable in size to the contribution expected from the QCD evolution equation. For convenience we will introduce the ratio R_L defined as follows:

$$R_L = \frac{\sigma_L(\gamma^* + p \to X + p)}{\sigma_L^{tot}(\gamma^* + p)} \ .$$

Requiring $R_L \leq 1$ and assuming that for $Q^2 = 10$ GeV^2

$$\sigma_L^{tot}(\gamma^* + p) \leq 0.5\, \sigma_T^{tot}(\gamma^* + p) \tag{45}$$

the inconsistency of the leading $\alpha_S \ln x$ approximation and the evolution equation should occur at $x \leq 10^{-6}$. In practice one should require a more severe limit on R_L, since the diffraction cross section is always a small part of the total cross section especially in the limit of black interactions. Let us take for illustration $R_L = 0.2$ as the limit. In this case the slowing down of structure functions increase should occur for $x \sim\leq 10^{-4.3}$.

There is a certain similarity between these estimates and the estimates exploring the increase with $\frac{1}{x}$ of shadowing corrections to the QCD evolution equation which were calculated within the BFKL approximation. In [59] shadowing corrections were estimated within the constituent quark model with the radius of the constituent quark equal to $\frac{1}{2.5}$ GeV^{-1}. In QCD the value of shadowing corrections calculated in [60] by iterating the hard amplitude depends strongly on the fitting parameter – the correlation radius of gluons in a average configuration in the wave function of a hadron. Theoretical calculations made in [60] found that for realistic parameters, corresponding to a correlation radius comparable to the radius of a hadron, the value of hard shadowing corrections to parton distributions is negligible in the kinematical range of HERA. (For recent numerical calculations see [62, 65]). The major difference between our estimate and the one implied by shadowing corrections is that we consider cross sections of coherent diffractive dissociation into small masses which includes the nonperturbative QCD effects in a different and rather reliable way. The derivation of the region of applicability of the leading $\alpha_s \ln x$ approximation and/or evolution equation for the cross section of longitudinally polarized photons is based on equations which use experimentally measurable quantities.

An estimate of where the consistency of QCD expectations fails can also be obtained from the consideration of the ratio of cross sections for the diffractive production of small masses and for the inclusive diffractive production $\sigma_D(\gamma^* + p)$,

$$R_D = \frac{\sigma_L(\gamma^* + p \to X + p)}{\sigma_D(\gamma^* + p)} \ .$$

The ratio R_D should be smaller than 1. From the discussion presented in this lecture we

expect,

$$R_D \propto \frac{[xG_p(x,Q^2)]^2}{Q^4 F_{2p}(x,Q^2)} \ .$$

Assuming that $R_D = \ 0.1$ at $Q^2 = 10$ GeV^2 and $x = 10^{-3}$ and using the new CTEQ3L parameterization [63] we obtain $R_D = 1$ for $x \sim 10^{-5.5}$ (see figure 5).

If one were to use the BFKL prediction for the rise of gluons (with an intercept of the BFKL Pomeron of 1.7 at $Q^2 = 10$ GeV^2 [8]), which is faster than that of the CTEQ parameterization, the result would be that $R_D = 1$ at $x = 10^{-4.4}$.

The value $R_D = 1$ which we used to deduce this restriction is unrealistically large since ρ meson production is one of many possible channels for the fragmentation of a $q\bar{q}$ pair. We thus expect that the fast increase of the cross section for hard diffractive processes should stop at much larger x. Assuming a plausible value for R_D, $R_D = 0.4$, the slow down should occur around $x \sim 10^{-4}$ or even earlier. Note that in QCD the cross sections for hard diffractive production of states X with $M_X^2 \ll Q^2$ should have the same x dependence, independent of M_X.

It is also interesting to note that we overestimate the value of $1/x$ since we ignore other higher twist diffractive processes which decrease slower with Q^2 (cf. discussion in section 10). The contribution of hard diffraction dissociation into large masses M^2 ($Q^2 \leq M^2$) has been also ignored in the above analysis. Hard diffraction dissociation into large masses has been recently estimated in PQCD in [57] in the triple Pomeron limit. Including this term would lead to a more stringent restriction on the region of applicability of QCD evolution equation and/or leading $\alpha_s \ln x$ approximation. Thus our conclusion is that violation of leading logarithms approximation is expected in a range of x which is in the reach of accelerators such as HERA or LHC.

We shall now deduce a more stringent restriction on the increase of parton distributions based on the interaction picture in the laboratory frame. We consider here the scattering of a small object, a $q\bar{q}$ pair, from a large object, a nucleon. If only hard physics was relevant

[8] In the expression for the intercept of the singularity corresponding to the BFKL Pomeron, $n = 1 + \frac{12\alpha_s \ln 2}{\pi}$, we chose $\alpha_s(Q^2 = 10 \text{ GeV}^2) = 0.25$ which leads to $n(Q^2 = 10 \text{ GeV}^2) = 1.7$.

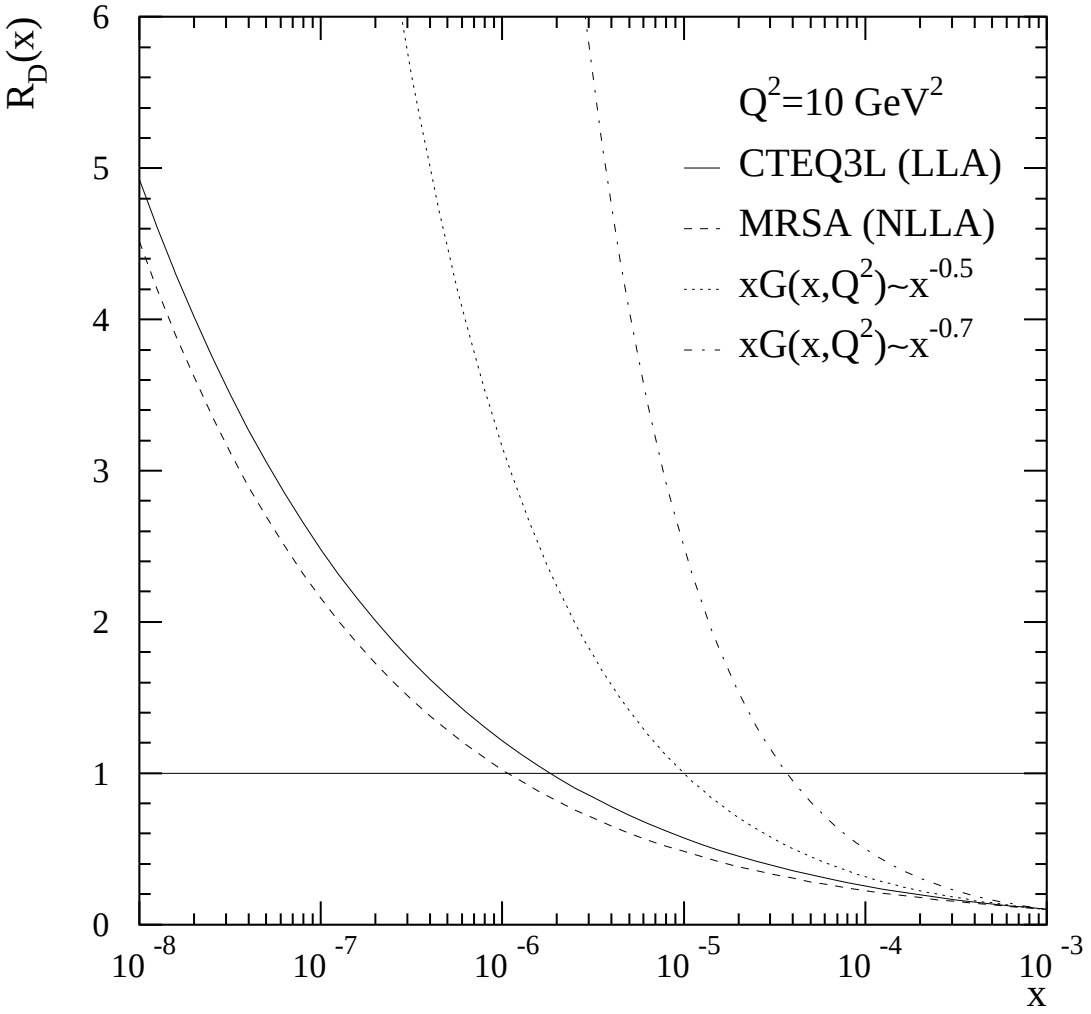

Figure 5: The ratio $R_D \sim \frac{(xG(x,Q^2))^2}{Q^4 F_2}$ normalized to be 0.1 at $x = 10^{-3}$ at $Q^2 = 10$ GeV^2 for two different parameterizations of parton distributions and obtained assuming $xG(x,Q^2) \sim x^n$ as indicated in the figure.

for the increase of parton distributions at small x, the radius of a nucleon should not increase (small Gribov diffusion). Under this assumption the unitarity limit corresponds to a black nucleon. In this case the inelastic cross section cannot exceed the geometrical size of the nucleon

$$\sigma(q\bar{q}N) = \frac{\pi^2}{3} b^2 \alpha_s(1/b^2) x G_N(x, b^2) < \pi r_N^2 \ . \tag{46}$$

To find the value of r_N in eq.(46) we use the optical theorem to calculate the elastic cross section for a $q\bar{q}$ pair scattering off a nucleon,

$$\sigma_{el} = \frac{\sigma_{tot}^2}{16\pi B} \tag{47}$$

where B is the slope of the elastic amplitude (cf. discussion in section 4). To deduce the inequality (46) we assume that the interaction of a $q\bar{q}$ pair with a target is black and therefore the elastic cross section is equal to the inelastic cross section $\sigma_{el} \leq \sigma_{inel}$. Based on this we find $r_N^2 = 4B \simeq 16$ GeV$^{-2} \simeq (0.8$ fm$)^2$ is the radius of a nucleon. It follows from the above equations that practically the same estimate is obtained from the assumption that $\frac{\sigma(el)}{\sigma(tot)} \sim (0.3 - 0.5)$.

According to our estimate (in sections 4 and 5) for $Q^2 = 10$ GeV^2, $\quad b = 0.3$ fm at least for higher twist effects. If we then determine at which x the geometrical cross section is saturated we obtain for $b = 0.3$ fm and $\alpha_s(Q^2 = 10 \text{ GeV}^2) = 0.3$, $xG_p(x, Q^2 = 10 \text{ GeV}^2) \leq 43$. If for illustration we use a parameterization $xG_p(x, Q^2) = 4/3x^{-0.36}$ which is consistent with the current data we find that $x \geq 6.0\ 10^{-5}$. Similar consideration for the case of scattering off nuclei leads to

$$\frac{1}{A} x G_A(x, Q^2 = 10 \text{ GeV}^2) \leq \frac{43}{A^{1/3}} \tag{48}$$

Restriction (48) has obvious practical implications for nucleus-nucleus collisions at LHC energies. In particular, it strongly affects theoretical predictions of the cross section of the minijet, and heavy quark production say for $Q^2 = 10 GeV^2$ and $x \leq 10^{-3}$.

The use of the amplitude for $q\bar{q}$ pair scattering off a nucleon to deduce the limit allows to account accurately for nonperturbative QCD effects through the unitarity condition for

such an amplitude. On the other hand if the increase of parton distributions is related to soft physics as well then the cross section may be allowed to increase up to smaller x values.

The black disc limit for $\sigma_{\gamma^* N}$ has been discussed earlier (for a review and references see [62, 64]). The difference compared to previous attempts is that we deduce the QCD formulae for the cross section of a $q\bar{q}$ pair scattering off a hadron target. For this cross section the geometrical limit including numerical coefficients unambiguously follows from unitarity of the S-matrix, that is the geometry of the collision. As a result we obtain an inequality which contains no free parameters. Recently a quantitative estimate of the saturation limit was obtained [66] by considering the GLR model [59, 60] of nonlinear effects in the parton evolution and requiring that the nonlinear term should be smaller than the linear term. The constraint obtained for $xG_p(x, Q^2)$ is numerically much less restrictive compared to our result. Even a more stringent restriction follows for the interaction of a colorless gluon pair off a nucleon from the requirement that the inelastic cross section for the scattering of a small size gluon pair should not exceed the elastic one

$$\sigma(ggN) = \frac{3\pi^2}{4} b^2 \alpha_s(1/b^2) x G_N(x, b^2) < \pi r_N^2 \ . \tag{49}$$

For $b = 0.25$ fm the geometrical limit is achieved for $x \sim 10^{-3}$.

We want to point out that the black disc limit implies a restriction on the limiting behavior of the cross sections for hard processes but does not allow to calculate it. The dynamical mechanism responsible for slowing down of the increase of parton distributions so that they satisfy equations (46, 49) is not clear. In particular the triple Pomeron mechanism for shadowing suggested in [59] does not lead to large effects at HERA energies especially if one assumes a homogeneous transverse density of gluons [64, 65].

The theoretical analysis performed in this section does not allow to deduce restrictions on the limiting behavior of parton distributions in a hadron. Beyond the evolution equation approximation and/or leading $\alpha_s \ln x$ approximation the restriction on the cross sections of deep inelastic processes cannot be simply expressed in terms of parton distributions in a hadron target.

We want to draw attention to the fact that nonperturbative QCD effects play an important role in the contribution of higher twist effects to $\sigma_L(\gamma^* p)$. This is evident from the impact parameter representation of the contribution to $\sigma_L(\gamma^* + p)$ of n consecutive rescatterings of small transverse size $q\bar{q}$ pairs. This contribution is proportional to

$$Q^2 \int |\psi^*_{\gamma_L}(z, b^2)|^2 dz d^2b \left[\alpha_s(1/b^2) b^2 x G(x, b)\right]^n \ .$$

The inspection of this integral shows that for large $n \geq 3$, b which dominates under the integral does not decrease with increasing Q^2 for $x \sim 10^{-3} \div 10^{-4}$. We use as estimate $xG_N(x, Q^2) \propto \sqrt{Q}$ which follows from the evolution equation for small x. (This QCD effect is absent in the applications [24] of the constituent quark model). Thus if higher twist effects were really important in small x physics, it would imply that the small x physics is the outcome of an interplay of hard (small b) and soft (large b) QCD. To illustrate this point let us consider the cross section of diffractive electroproduction of hadrons with masses $M^2 \sim Q^2$ by transversely polarized photons. Applying the same ideas as in the case of longitudinally polarized photons we would obtain a similar expression as given by equation 43. The important difference is that the wave function of a transversely polarized photon is singular for $z \to 0$ or 1. As a result the contribution of large impact parameters b in the wave function of the photon should give the dominant contribution to the integral in a wide kinematical range of x and Q^2. This has been understood long ago – see discussion in sections 13-14. A similar conclusion has been achieved recently [24] within the constituent quark model. (Note however that this model ignores the increase of gluon distribution with Q typical for QCD and therefore overestimates the nonperturbative QCD contribution). Thus such type of diffractive processes should depend on energy in a way similar to the usual soft hadron processes.

A good example of the consequences of the interplay of small b and large b physics is that in electroproduction of small mass states the unitarity limit may become apparent at larger x than in the case of the total cross section of deep inelastic processes.

12 Geometrical limit.

The important role of nonperturbative QCD effects clearly shows that new ideas beyond PQCD approach are required.

The starting point of our discussion is the observation that when l_c considerably exceeds the diameter of a target which is at rest, the virtual photon transforms into hadron components well before the target. Thus small x physics probes the interaction of various hadron wave packets with a target (for the sake of the argument we will consider the interaction with a proton target). The geometrical limit for the cross section of virtual photon scattering off a nucleon target will follow from the assumption that a target is black for the dominant hadron components in the wave function of the virtual photon. In this approximation, the structure functions of a target can be unambiguously calculated. A comparison with the formula deduced from the geometrical limit will imply certain restrictions on the increase of structure functions [67].

Blackness of hadron interactions at high energies has been predicted in the elastic eikonal models with input cross sections increasing with energy (see [68] and references therein). The assumption on the blackness of hadron-hadron interactions at high energies is often used to deduce the Froissart limit.

Under the assumption that the interaction is black, the cross section of non-diagonal diffractive processes should be small and decrease with increase of energy. This has been understood long ago by considering the example of an energetic particle scattering off a black potential well (see e.g. [69]).

Within this picture, in the limit $x \to 0$, the deep inelastic lepton scattering off a nucleon can be unambiguously calculated through the cross section of the reaction $e^+e^- \to$ hadrons [70],

$$\sigma_{inel}(\gamma^* + p) = \frac{\alpha}{3\pi} \langle\sigma\rangle \int\limits_{m_0^2}^{M_{max}^2} R(m^2) \frac{m^2}{(m^2+Q^2)^2} dm^2 \ , \tag{50}$$

where $\langle\sigma\rangle$ is the average interaction cross section, m denotes the mass of the state con-

tributing to the deep inelastic cross section and at the same time the center of mass energy of the e^+e^- system, m_0^2 is the hadronic scale ~ 1 GeV^2 and R is defined by

$$R(m^2) = \frac{\sigma(e^+e^- \to \text{hadrons})}{\sigma(e^+e^- \to \mu^+\mu^-)} \ . \tag{51}$$

The upper limit in formula (50), $M^2_{max} \sim Q^2(\frac{1}{mr_N} - 1)$ with r_N the radius of a nucleon, follows from the condition that the diffractive production of a state with mass m should not be suppressed by the nucleon form factor. Thus

$$\sigma(\gamma^* + p) = P_{had} \langle\sigma\rangle \ , \tag{52}$$

where the probability of a given configuration P_{had} is expressed by

$$P_{had} = \frac{\alpha}{3\pi} \int R(m^2) \frac{m^2}{(m^2 + Q^2)^2} dm^2 \ . \tag{53}$$

Since large masses dominate in the integral it is legitimate to substitute $R(m^2)$ by its asymptotic value. For numerical estimates we will use R for the case of 5 flavors, $R = \frac{11}{3}$. Thus in the unitarity limit

$$P_{had} = \frac{\alpha}{3\pi} R \left[\ln(\frac{1}{10x}) - 1\right] \ . \tag{54}$$

In the integral over m^2 we use the conventional definition of diffraction as leading to hadronic final states with $\frac{M_X^2}{s} \leq 0.1$ where diffractive production is not suppressed by the nucleon form factor.

The expression for F_{2p} follows from equations (52) and (53) and the relation between the total $\gamma^* p$ cross section and the structure function F_2

$$F_{2p}(x, Q^2) = \frac{Q^2 \langle\sigma\rangle}{12\pi^3} R \left[\ln \frac{1}{10x} - 1\right] \ . \tag{55}$$

For the proton target following [67] we estimate

$$\langle\sigma\rangle = \sigma_{pp}/2 \ . \tag{56}$$

For further estimates we shall use a parameterization of $F_{2p}(x, Q^2)$ given by expression (1).

Assuming that F_{2p} cannot exceed the unitarity limit given by (55) and taking $\langle\sigma\rangle =$ 40 mb allows to obtain some constraints on the region where parton distributions may increase with Q and $\frac{1}{x}$ [67]. Assuming that the parameterization given by (1) holds down to extremely low x, the geometrical limit would be exceeded at $x \sim 10^{-7},\ 10^{-8}$ for $Q^2 = 10$ GeV^2. This is three orders of magnitude below the present kinematical limit at HERA. The restrictions obtained from the geometrical limit for the cross section averaged over impact parameters are thus interesting from a purely theoretical point of view but not for any practical purposes. Somewhat more useful restrictions on the small x behavior follow from the mismatch of QCD predictions for inclusive and exclusive processes and from S-matrix unitarity constraint.

13 Diffraction in DIS at intermediate Q^2

It has been understood long ago that the production of almost on mass shell quarks by virtual photons should give a significant contribution to the total cross section for deep inelastic scattering at small x [71]. One of the predictions of this approach (which is essentially the parton model approximation) is a large cross section for diffractive processes. The QCD Q^2 evolution does not change this physical picture radically. The only expected modification of the picture is the appearance of a number of hard jets in the current fragmentation region [10] typical for including $\alpha_S \ln Q^2$ terms. It is often stated that the dominance of the BFKL Pomeron in diffractive processes predicts the dominance of final states consisting of hard jets [56, 72]. However this prediction is not robust since the analysis of Feynman diagrams for hard processes in QCD finds strong diffusion effects into the region of small transverse momenta of partons (see [57] and references therein). Recent HERA data [8] seem to support the picture with a dominance of events with small k_t. Thus it seems worthwhile to investigate the role of nonperturbative QCD physics in diffractive processes.

The interaction of a virtual photon with a target at intermediate Q^2 and small x, when

gluon radiation is negligible, can be considered as a transformation of γ^* into a $q\bar{q}$ pair which subsequently interacts with the target. In this case an important role is played by the quark configurations in which the virtuality of the quark interacting with the target is small,

$$k_{qt} \sim k_{t0} \ , \quad \alpha_q = \frac{(m_q^2 + k_{qt}^2)}{Q^2} \ . \tag{57}$$

Here α_q denotes the light-cone fraction of the photon momentum carried by the slower quark and k_{t0} is an average transverse momentum of partons in the hadron wave function, typically $k_{t0} \sim 0.3 - 0.4$ GeV.

In the language of non-covariant perturbation theory the $q\bar{q}$ configurations described by (57) correspond to an intermediate state of mass $m^2 \sim Q^2$ and of transverse size $\sim \frac{1}{k_{t0}} \geq 0.5$ fm. These configurations constitute a tiny fraction $\sim \frac{k_{qt}^2}{Q^2}$ of the phase volume kinematically allowed for the $q\bar{q}$ pair. However the interaction in this case is strong – similar to the interaction of ordinary hadrons, since the virtuality of the slower quark is small and the transverse area occupied by color is large. The contribution of these configurations leads to Bjorken scaling since the total cross section is proportional to $\frac{1}{Q^2}$ and in the parton model only these configurations may contribute to the cross section. Hence Bjorken has assumed [71] that all other configurations are not important in the interaction though the underlying dynamics of such a suppression was not clear at that time [73]. Accounting for the $(\frac{k_{qt}^2}{Q^2})$ factor in equation (50) allowed him to reconcile the Gribov dispersion representation with scaling. He suggested to refer to these configurations as aligned jets since both quarks have small transverse momenta relative to the photon momentum direction. In further discussions we will refer to this approach as that of the Aligned Jet Model (AJM). Note that in terms of the Feynman fusion diagram the aligned jet contribution arises only for transversely polarized virtual photons. This is because the vertex for the transition $\gamma_T^* \to q\bar{q}$ is singular $\sim \frac{1}{z}$ when the fraction of the photon momentum z carried by the slowest quark (antiquark) tends to 0. For the case of a longitudinally polarized photon the aligned jet approximation produces results qualitatively different from expectations in QCD where the contribution of symmetric jets dominates.

This is because in QCD the dominant contribution to the γ_L^*–nucleon cross section arises from the region of large $k_{qt} \sim \frac{Q}{2}$.

In QCD the interaction of quarks with large relative transverse momenta with a target is suppressed but not negligible. The suppression mechanism is due to color screening since $q\bar{q}$ configurations with large k_t correspond, in the coordinate space, to configurations of small transverse size, $b \sim \frac{1}{k_t}$, for which equation (8) is applicable. It is easy to check that the contribution of large k_t also gives a scaling contribution to the cross section. The practical question then is which of the two contributions dominates at intermediate $Q^2 = Q_0^2 \approx 4$ GeV^2, above which one can use the QCD evolution equations. To make a numerical estimate we assume that the $q\bar{q}$ configurations with $k_{qt} \leq k_{t0}$, in which color is distributed over a transverse area similar to the one occupied by color in mesons, interact with a cross section similar to that of the pion. A comparison with experimental data for $F_{2p}(x \sim 0.01, Q_0^2)$ indicates that at least half of the cross section is due to soft, low k_t interactions [10, 37]. A crucial check is provided by applying the same reasoning to scattering off nuclei in which the interaction of the soft component should be shadowed with an intensity comparable to that of pion-nucleus interaction. Indeed the current deep inelastic data on shadowing for $F_{2A}(x, Q^2)$ are in reasonable agreement with calculations based on the soft mechanism of nuclear shadowing [10, 11].

Similarly to the case of hadron-nucleon and hadron-nucleus interactions, the interaction of γ^* in a soft hadron component naturally leads to diffractive phenomena. Application of the Gribov representation with a cutoff on the k_t of the aligned jets in the integral leads to a diffractive mass spectrum for the transversely polarized virtual photon [73]

$$\frac{d\sigma}{dM^2} \propto \frac{1}{(M^2 + Q^2)^2} \ . \tag{58}$$

The two major differences compared to the hadronic case are that elastic scattering is substituted by production of states with $\langle M^2 \rangle \approx Q^2$ and that the contribution of configurations of small spatial size is larger for γ_L^*.

If the aligned jet configurations were dominant, the fraction of cross section of deep

inelastic $\gamma^* N$ scattering due to single diffractive processes would be

$$R^{\rm AJM}_{\rm single\ dif} = \sigma_{\rm dif}/\sigma_{\rm tot} = \frac{\sigma_{\pi N}({\rm el}) + \sigma_{\pi N}({\rm dif})}{\sigma_{\pi N}({\rm tot})} \sim 0.25 \quad . \tag{59}$$

Our numerical estimates indicate that for $Q^2 \sim Q_0^2$ and $x \sim 10^{-2}$ the AJM contributes about $\eta \sim 60 - 70\%$ of the total cross section. So we expect that in this Q^2 range the probability for diffraction is

$$R_{\rm single\ dif} = \eta R^{\rm AJM}_{\rm single\ dif} \sim 15\%. \tag{60}$$

This probability is actually related in a rather direct way to the amount of shadowing in interactions with nuclei in the same kinematic regime, so it is quite well determined by the nuclear shadowing data.

To estimate the probability of events with large rapidity gaps one has to add the processes of diffractive dissociation of the nucleon and double diffraction dissociation, leading to an estimate

$$P_{\rm gap} = (1.3 - 1.5) R_{\rm single\ diff} \sim 0.2 \ . \tag{61}$$

This is rather close to the observed gap survival probability for photoproduction processes [74].

The characteristic features of the AJM contribution which can be checked experimentally are the charge and flavor correlations between the fastest and the slowest diffractively produced hadrons which should be similar to those in $e^+e^- \to$ hadrons at $M^2 \sim Q^2$.

Another important feature of the soft contribution which distinguishes it from the contribution of hard processes is the t dependence of the cross section for $M^2 \leq Q^2$. Since the size of the configurations is comparable to that of the pion one may expect that the t slope of the cross section, B, should be similar to that of the pion-nucleon interaction, i.e. $B \geq 10$ GeV^{-2} which is much softer than for hard processes where we expect $B \approx 4$ GeV^{-2} (see discussion in section 4). The large value of the slope for the soft component is also natural in the parton type logic where only slow partons interact. It is easy to check that for $-t \gg k_{t0}^2 \sim 0.1$ GeV^2 the mass of the produced hadron system is larger than the

mass of the intermediate state by factor $\frac{\sqrt{-t}}{k_{t0}}$. Thus for large t the production of masses $M \leq Q$ is suppressed. Therefore the study of the t-dependence of diffraction can be used to disentangle the contribution of soft and hard mechanisms.

This discussion indicates also that the contribution of non-diagonal transitions "M^2" $\rightarrow$ "M'^2 leads to a weaker decrease of the differential cross section with M^2 than given by equation (58). Besides at large $M^2 \sim$ *few* Q^2 one expects an onset of the dominance of the triple Pomeron mechanism which corresponds to

$$\frac{d\sigma}{dM^2} \propto \frac{1}{Q^2 M^2}. \tag{62}$$

14 Q^2 evolution of the soft contribution in diffraction.

The major difference between the parton model and QCD is the existence in QCD of a significant high p_t tail in the parton wave functions of the virtual photon and the proton. This is the source of the violation of Bjorken scaling observed at small x. It is thus necessary to modify the aligned jet model to account for the hard QCD physics.

It is in general difficult to obtain with significant probability a rapidity gap in hard processes in perturbative physics. Confinement of quarks and gluons means that a gap in rapidity is filled by gluon radiation in PQCD and subsequently by hadrons [75]. It is possible to produce diffraction in perturbative QCD but the price is a suppression by powers of the coupling constant α_s and/or powers of Q^2. In first approximation in calculating diffraction in deep inelastic processes at small x we will thus neglect diffraction in PQCD. In the following analysis, for the description of large rapidity gap events, we shall use the QCD modification of the AJM model suggested in [10] as well as the suggestion of Yu. Dokshitzer [76] to add to the conventional evolution equation the assumption of local duality in rapidity space between quark-gluon and hadron degrees of freedom.

In the course of the following considerations it will be convenient to switch to the Breit frame. In this frame the photon has momentum $(0, -2xP)$ and the initial proton has momentum (P,P). Correspondingly $Q^2 = 4x^2P^2$. The process of diffraction can be

viewed as the virtual photon scattering off a color singlet $q\bar{q}$ pair with the interacting parton carrying a light-cone fraction α and the spectator parton carrying a light-cone fraction x_1. We assume here the local correspondence in rapidity space between partons and hadrons. The mass of the produced system, M is given by

$$M^2 = (p_{\gamma^*} + p_{x_1} + p_\alpha)^2 = P^2((\alpha + x_1)^2 - (\alpha + x_1 - 2x)^2) = \\ Q^2 + 4P^2(\alpha + x_1)x = Q^2\frac{\alpha + x_1 - x}{x} \ . \tag{63}$$

In the approximation that gluon radiation is neglected (parton model) $\alpha = x$ and the mass of the diffractively produced system M is

$$M^2 = Q^2 x_1/x \ . \tag{64}$$

The differential cross section for production of mass M follows from equation (58),

$$\frac{d\sigma^{\rm AJM}}{dM^2} = \Gamma \int dx_1 \delta(x_1 - \frac{xM^2}{Q^2})\frac{1}{(Q^2 + M^2)^2} = \\ \frac{\Gamma}{Q^4}\int dx_1 \delta(x - \alpha)\delta(x_1 - \frac{xM^2}{Q^2})\frac{1}{(1 + x_1/x)^2} \ . \tag{65}$$

Here Γ is the factor which includes the density of correlated color singlet pairs and the cross section for interaction of the photon with the parton. The total cross section for diffractive dissociation comes out to be proportional to $\frac{1}{Q^2}$,

$$\int \frac{d\sigma^{AJM}}{dM^2} dM^2 = \frac{\Gamma}{Q^2}\int \frac{dx_1}{x}\frac{1}{(1 + x_1/x)^2} = \frac{\Gamma}{Q^2} \ . \tag{66}$$

We do not restrict the integration over x_1 in equation (66) since the major contribution comes from the region of $x_1 \sim x$. Thus we can formulate diffraction in the infinite momentum frame as a manifestation of short rapidity range color correlation between partons in the nonperturbative parton wave function of the nucleon. To calculate the Q^2 evolution in QCD we have to take into account that the parton with momentum fraction α has its own structure at higher Q^2 resolution and that the γ^* scatters off constituents of the "parent" parton. This is the usual evolution with Q^2 which can be accounted for

in the same way as in the QCD evolution equations by the substitution

$$\Gamma\delta(x-\alpha) \rightarrow P\sum_j e_j^2 d_j^{\rm pert}(\frac{x}{\alpha},Q^2,Q_0^2)$$

where $d_j^{\rm pert}(x,Q^2,Q_o^2)$ are the structure functions of the parent parton. This effect leads to the change of the relationship between x_1 and x resulting from parton bremsstrahlung,

$$\frac{d\sigma^{\rm soft+QCD}}{dM^2} = \frac{P}{Q^4}\int dx_1 \int \frac{d\alpha}{\alpha}\sum_j e_j^2 d_j^{\rm pert}(\frac{x}{\alpha},Q^2,Q_0^2) d_j^{\rm nonpert}(\alpha,Q_0^2)$$
$$\delta(x_1+\alpha-x-\frac{xM^2}{Q^2})\frac{1}{x}\frac{1}{(1+x_1/x)^2}\theta(\lambda-\frac{\alpha+x_1-x}{1-x}) \ . \qquad (67)$$

P denotes the probability of diffractive scattering in a soft interaction and $d_j^{\rm nonpert}(\alpha,Q_0^2)$ is the parton distribution in the soft component producing diffraction (compare discussion in the previous section). The θ function term reflects the condition that diffraction in the nonperturbative domain is possible only for

$$0 \leq \frac{M^2}{s} = \frac{Q^2(\alpha+x_1-x)}{x(\nu-Q^2)} = \frac{\alpha+x_1-x}{(1-x)} \equiv \lambda \sim 0.05-0.1 \ . \qquad (68)$$

After performing the integral over x_1 we can rewrite equation (67) in the form

$$\frac{d\sigma^{\rm soft+QCD}}{dM^2} = \frac{P}{Q^4}\int_x^1 \frac{d\alpha}{\alpha}\sum_j e_j^2 d_j^{\rm pert}(\frac{x}{\alpha},Q^2,Q_0^2) d_j^{\rm nonpert}(\alpha,Q_0^2)$$
$$\frac{1}{(2-\alpha/x+M^2/Q^2)^2}\theta\left(\lambda(1-x)-\frac{xM^2}{Q^2}\right)\theta\left(1-\frac{\alpha}{x}+\frac{M^2}{Q^2}\right) \ . \qquad (69)$$

After integrating equation (69) over the mass of the produced system, we obtain for the total diffractive cross section

$$\sigma^{\rm soft+QCD} = \frac{P}{Q^2}\int_x^1 \frac{d\alpha}{\alpha}\sum_j e_j^2 d_j^{\rm pert}(\frac{x}{\alpha},Q^2,Q_o^2) d_j^{\rm nonpert}(\alpha,Q_0^2)$$
$$\frac{x-\alpha+\lambda(1-x)}{2x-\alpha+\lambda(1-x)}\theta(\lambda(1-x)-(\alpha-x))$$
$$. \qquad (70)$$

14.1 Evolution equation for diffraction.

Let us rewrite equation (67) in a form more convenient for the application of the evolution equations. To this end let us consider the ratio

$$R \equiv Q^2 \frac{d\sigma^{\rm soft+QCD}}{d\frac{M^2}{Q^2}}$$

and analyze the Q^2 evolution of the diffraction cross section at **fixed** $\kappa = M^2/Q^2$. Neglecting the valence quark contribution and calculating leading $\alpha_s \ln \frac{Q^2}{Q_o^2}$ corrections to equation (70) we find,

$$\begin{aligned} \frac{\partial}{\partial \ln Q^2} R(x,Q^2) = P \int_x^1 \frac{d\alpha}{\alpha} \left\langle e_j^2 \right\rangle \\ \left\{ P_{qq}(\frac{x}{\alpha}, Q^2) 2S(\alpha, Q^2) + N_f P_{qg}(\frac{x}{\alpha}, Q^2) G(\alpha, Q^2) \right\} \\ \theta\left(\lambda(1-x) - xk\right) \\ \theta\left(1 - \frac{\alpha}{x} + k\right) \\ f(\kappa, \alpha, x) \ , \end{aligned} \tag{71}$$

where $\left\langle e_j^2 \right\rangle$ is the average quadratic electric charge of partons and

$$f(\kappa, \alpha, x) = (\kappa + 2 - \alpha/x)^{-2}$$

for $\kappa \leq 2$. For larger κ where the triple Pomeron contribution is important $f \sim \kappa^{-1}$.

14.2 Qualitative pattern of x and Q^2 dependence of diffraction.

It is easy to see that equations (69,70,71) lead to the leading twist diffraction. To see the pattern of the x, Q^2 dependence we can assume that $d_j^{\rm pert}(x,Q^2) = \frac{d}{x^n}$ and $d_j^{\rm nonpert}(x,Q_0^2) = \frac{d_0}{x^{n_0}}$. It follows from equation (69) that for $x \ll \lambda$ the ratio $\frac{\sigma_{\rm diff}}{\sigma_{\rm tot}}$ does not depend on x. One can also see that the characteristic gap interval is

$$\Delta y = \ln \frac{s}{M m_p} = \ln \frac{s}{Q^2} + \ln \frac{Q^2}{M\ m_p} = \ln \frac{1}{x} + \ln(\frac{Q^2}{M\ m_p}) \ . \tag{72}$$

The second term $\ln \frac{Q^2}{M\ m_p}$ increases with Q^2 in the parton model, while the scaling violation tends to reduce this increase since the mean value of M^2/Q^2 at fixed x increases with Q^2.

There are several qualitative differences between the QCD improved soft diffraction and the parton model (AJM).

(i) Due to QCD evolution the number of diffractively produced hard jets and the average transverse momentum of diffractively produced hadrons should increase with Q^2.

(ii) The distribution of $\frac{M^2}{Q^2}$ becomes broader in QCD with increasing Q^2.

(iii) While in the parton model the cross section for the interaction of the longitudinally polarized virtual photon is a higher twist effect, in QCD diffraction is a leading twist for any polarization of the virtual photon. The final state in the case of longitudinally polarized photons should contain at least 3 jets, two of them should have large transverse momenta comparable with Q.

14.3 Connection with the Ingelman-Schlein Model

Ingelman and Schlein have suggested to treat hard diffractive processes using the concept of parton distribution in the Pomeron [52]. In this approach one calculates the light-cone fraction of the target carried by the Pomeron, x_P, and light-cone fractions of the Pomeron momentum carried by quarks and gluons, β. It is assumed that parton distributions in the Pomeron, $\beta q_P(\beta, Q^2), \beta g_P(\beta, Q^2)$ are independent of x_P and the transverse momentum of the recoil nucleon. For the process of inclusive deep inelastic diffraction β is simply related to the observables,

$$\beta = \frac{Q^2}{Q^2 + M_X^2} \tag{73}$$

The Q^2 evolution of the total cross section of diffraction as considered in the previous subsections is consistent with the expectation of the Ingelman-Schlein model (though the final states are not necessarily the same). The aligned jet model in this case serves as a boundary condition defining parton distributions in the Pomeron at intermediate Q_0^2 above which QCD evolution takes place. The aligned jet model corresponds to the quark

distribution in the Pomeron

$$\beta q_P(\beta, Q_0^2) \propto \beta. \tag{74}$$

It follows from the discussion in the end of section 13 that taking into account the non-diagonal transitions in the aligned jet model and the triple Pomeron contribution would make the distribution flatter. A similar, rather flat, distribution is expected for gluons for these Q^2. This expectation of the aligned jet model is different from the counting rule anzatz of [52]: $\beta q_P(\beta, Q_0^2) \propto (1-\beta)$.

15 Non-universality of the pomeron in QCD.

Theoretical considerations of soft diffractive processes have demonstrated that ordinary hadrons contain components of very different interaction strength [77, 16]. This includes configurations which interact with cross sections much larger than the average one and configurations which interact with very small cross sections, described by equation (8) for a meson projectile. The probability distribution to find a pion and nucleon in configurations with a given interaction cross section σ – $P(\sigma)$ is presented in figure 6 [16], which also includes the estimate of the probability of small cross sections in the pion which is close in spirit to the analysis of the diffractive ρ meson production described in this report.

The presence in hadrons of various configurations of partons having different interaction cross sections with a target is in evident contradiction with the idea of a universal vacuum pole where universal factorization is expected. At the same time it is well known that the Pomeron pole approximation is not self-consistent. The vacuum pole should be accompanied by a set of Pomeron cuts [15]. For the sum of the Pomeron pole and the Pomeron cuts no factorization is expected. Thus the S matrix description and the QCD description are not in variance. We shall enumerate now where and how to search for the non universality of the effective Pomeron understood as the sum of the pomeron pole and the Pomeron cuts.

It is natural to distinguish two basic manifestations of the non universality of the

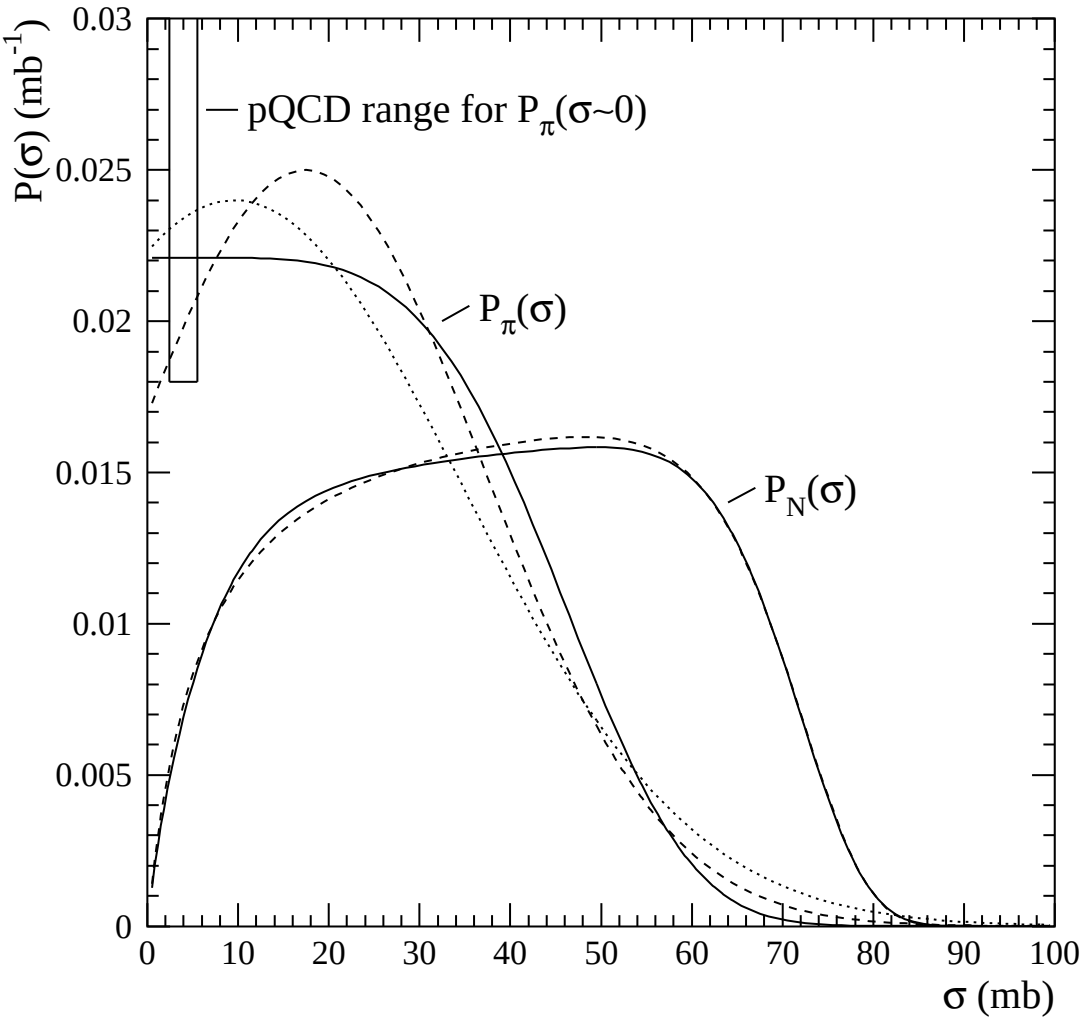

Figure 6: Cross-section probability for pions $P_\pi(\sigma)$ and nucleons $P_N(\sigma)$ as extracted from experimental data. $P_\pi(\sigma \sim 0)$ is compared with the perturbative QCD prediction.

effective Pomeron trajectory, $\alpha_{\mathcal{P}}(t) \approx \alpha_0 + \alpha' t$, a different energy dependence of the interaction cross section, which is characterized by a different value of α_0, and a different rate of the Gribov diffusion, which would manifest itself in different values of α'.

15.1 Non-universality of the energy dependence.

To study the non universality of α_0 it is necessary to study the energy dependence of the electroproduction of vector mesons as a function of Q^2. Up to now only two results are known, $\alpha_0 \sim 1.08$ from the ρ meson photoproduction [78], and $\alpha_0 \sim 1.30$ as estimated from preliminary HERA data at $Q^2 \sim 10$ GeV^2 [5]. The key question is at what Q^2 a significant rise of α_0 starts – this will give a direct information on the transition region from soft to hard physics. Optimists of PQCD suggest that the rise may occur already at $Q^2 \sim 3$ GeV^2. The same question applies for production of heavier ϕ and J/Ψ mesons. Since the J/Ψ meson is a small object one may speculate that in this case the rise could start already for photoproduction (the experimental data indicate that the slope of the J/Ψ exclusive photoproduction cross section is close to the value given by the two-gluon form factor of the nucleon). The practical problem for a quantitative analysis is that no accurate data on **exclusive** J/Ψ photoproduction at fixed target energies are available at the moment. Inclusive fixed target data where the J/ψ meson carries practically the whole momentum of the projectile photon which are used to extract the exclusive channel seem to be significantly contaminated by the contribution of the reaction $\gamma + p \to J/\Psi + X$ which is peaked at $x_F \equiv p_v/p_\gamma$ close to 1.

15.2 Non-universality of the t-dependence.

The slope of the effective Pomeron trajectory α' should decrease with increasing Q^2. This is because the Gribov diffusion in the impact parameter space, which leads to finite α' [33], becomes inessential in the hard regime. This is a consequence of the increase with energy of the typical transverse momenta of partons. Thus for the reactions $\gamma^* + N \to V + N$ the effective α' should decrease with increasing Q^2 while a universal Pomeron exchange

approximation predicts for the energy dependence of the slope

$$B(s) = B(s_0) + 2\alpha' \ln\left(\frac{s}{s_0}\right) \tag{75}$$

with $\alpha' \sim 0.25$ GeV^{-2}.

It is possible to look for this effect by comparing the HERA and the NMC data on the ρ meson production. The universal Pomeron model predicts that the slope should change from $B \sim 4$ GeV^{-2} [4] to $B \sim 6$ GeV^{-2} at HERA energies while in the perturbative domain a much weaker change of the slope is expected.

The slope of the effective Pomeron trajectory α' may depend on the flavor. It should decrease with the mass of flavor. Thus it would be very important to measure the effective α' for the diffractive photoproduction of ρ, ϕ and J/Ψ. If PQCD is important for J/Ψ photoproduction one would expect a smaller increase of the slope with energy in this case.

15.3 Non-universality of the gap survival probability.

The presence of configurations of different size in hadrons (photons) should also manifest itself in the non universality of the gap survival probability in the two jet events. Since the probability of gap survival is determined by the intensity of the *soft* interaction of the projectile with the target, the survival probability should increase with increase of Q^2, and at fixed Q^2 it should be larger for the heavy $q\bar{q}$ components of the photon. Also, the gap survival probability in the photon case should be substantially larger than that observed in $p\bar{p}$ collisions at FNAL collider [79]. This reflects the difference between $\sigma_{tot}(p\bar{p}) \approx 80$ mb and the effective cross section for the interaction of the hadronic components of $\gamma(\gamma^*)$ with nucleon of ≤ 30 mb.

Observation of non-universalities discussed here will shed light on the structure of the effective Pomeron operating in strong interactions and will help to address the question about the major source of the increase of the total cross section of $p\bar{p}$ interaction — soft physics or hard physics of small size configurations.

15.4 Non-universality of diffraction dissociation

Since the object which couples to the nucleon in the hard coherent processes is different from soft Pomeron one may expect a difference between the value of the ratio $\left.\frac{\frac{d\sigma^{\gamma^*+p\to\rho+X}}{dt}}{\frac{d\sigma^{\gamma^*+p\to\rho+p}}{dt}}\right|_{t=0}$ and similar ratio for soft processes. Qualitatively, one may expect that since the coupling of effective Pomeron in hard processes is more local the ratio of diffraction dissociation and elastic cross sections should be substantially smaller for hard processes, at least for small excitation masses.

16 Summary.

We have demonstrated that color coherent phenomena should play in QCD a rather direct role both in the properties of hadrons and in the high energy collisions. It seems now that recent experimental data confirm some of the rather nontrivial predictions of QCD and help to elucidate such old problems as the origin of the Pomeron pole and the Pomeron cuts in the Reggeon Calculus. Thus we expect that the investigation of coherent hard and soft diffractive processes may be the key in obtaining a three dimensional image of hadrons, in helping to search for new forms of hadron matter at accelerators and in understanding the problem of inter-nucleon forces in nuclei. Forthcoming high luminosity studies of diffraction at HERA which will include among other things the detection of the diffracting nucleon and the $\sigma_L - \sigma_T$ separation would greatly help in these studies.

Acknowledgments

We would like to thank J. Bartels, J. Bjorken, S. Brodsky, W. Buchmuller, A. Caldwell, J. Collins, J. Ellis, G. Knees, H. Kowalski, L. Lipatov, A. Mueller, G. Wolf for the fruitful discussions of the interplay of soft and hard physics and of methods of their investigation. Many thanks go to R. Klanner for a careful reading of the text. We would also like to acknowledge the hospitality of DESY where part of this work was completed.

References

[1] L. L. Frankfurt, G. A. Miller and M. Strikman, Ann. Rev. of Nucl. and Particle Phys. 44 (1994) 501.

[2] ZEUS Collaboration, M. Derrick et al., Phys. Lett. B316 (1993) 412; Z. Phys. C65 (1995) 379.

[3] H1 Collaboration, I. Abt et al., Nucl. Phys. B407 (1993) 515.

[4] NMC Collaboration, P. Amaudruz et al., Z. Phys. C51 (1991) 387; M. Arneodo et al., CERN-PRE/94-146.

[5] M.Derrick et al., DESY-95-133, July 1995

[6] ZEUS Collaboration, M. Derrick et al., Phys. Lett. B315 (1993) 481.

[7] H1 Collaboration, T. Ahmed et al., Nucl. Phys. B429 (1994) 477.

[8] ZEUS Collaboration, M. Derrick et al., Phys. Lett. B332 (1994) 228.

[9] M. Arneodo, Phys. Rep. 240 (1994) 301.

[10] L. L. Frankfurt and M. Strikman, Phys. Rep. 160 (1988) 235.

[11] L. L. Frankfurt and M. Strikman, in "Modern Topics in Electron Scattering", Editors B. Frois and I. Sick, 1991, p.762, World Scientific.

[12] W. Mollet et al., Phys. Rev. Lett. 26 (1977) 1646; M. Zielinski et al., Z. Phys. C16 (1983) 197.

[13] V. N. Gribov, B. L. Ioffe and I. Ya. Pomeranchuk, Yad. Fiz. 2 (1965) 768; C. Llewellyn-Smith, Phys. Rev. D4 (1971) 2392.

[14] B. L. Ioffe, Phys. Lett. 30 (1968) 123.

[15] V. N. Gribov, in "Regge theory of low-p(T) hadronic interactions" Caneschi, L. (ed.) 1990, p 63-71; Sov. Phys. JETP 26 (1968) 414; Zh. Eksp. Teor. Fiz. 53 (1967) 654.

[16] B. Blättel, G. Baym, L. L. Frankfurt and M. Strikman, Phys. Rev. Lett. 71 (1993) 896.

[17] L. Frankfurt, G. A. Miller and M. Strikman, Phys. Lett. B304 (1993) 1.

[18] L.Frankfurt, W.Koepf, and M.Strikman, Preprint TAUP-2290-95, hep-ph/9509311.

[19] L. L. Frankfurt, A. Radyushkin and M. Strikman, in preparation.

[20] F. E. Low, Phys. Rev. D12 (1975) 163.

[21] S. Nussinov, Phys. Rev. Lett. 34 (1975) 1286.

[22] J. Gunion and D. Soper, Phys. Rev. D15 (1977) 2617.

[23] N. N. Nikolaev and B. G. Zakharov, Z. Phys. C53 (1992) 331.

[24] N. N. Nikolaev and . G. Zakharov, Landau-16/93 (1993)

[25] A. D. Martin, W. J. Stirling and R. G. Roberts, Phys. Rev. D50 (1994) 6734.

[26] J. C. Collins, J. Huston, J. Pumplin, H. Weerts and J. J. Whitmore, CTEQ/PUB/02; hep-ph/9406255.

[27] M. Glück, E. Reya and A. Vogt, Z. Phys. C53 (1992) 127.

[28] A. D. Martin, W. J. Stirling and R. G. Roberts, RAL–94–104.

[29] S. J. Brodsky, L. Frankfurt, J. F. Gunion, A. H. Mueller and M. Strikman, Phys. Rev. D50 (1994) 3134.

[30] A. Donnachie and P. V. Landshoff, Phys. Lett. 185B (1987) 403; Nucl. Phys. B311 (1989) 509.

[31] P. L. Frabetti et al., Phys. Lett. B316 (1993) 197; M. Binkley et al., Phys. Rev. Lett. 48 (1982) 73.

[32] A. E. Asratian et al., Z. Phys. C58 (1993) 55.

[33] V. N. Gribov, in "Regge theory of low-p(T) hadronic interactions", Caneschi L. (ed.) 1990, p. 22-23; JETP Lett. 41 (1961) 667; Yad. Fiz. 5 (1967) 399; Yad. Fiz. 9 (1969) 3; " Space-time description of hadron interactions at high energies", 1st ITEP school, v.I "Elementary particles", p. 65 (1973).

[34] V. N. Gribov, L. N. Lipatov, Yad. Fiz. 15 (1972) 781; Yad. Fiz. 15 (1972) 1213; Yu.L. Dokshitzer, Sov. Phys. JETP 46 (1977) 641; G. Altarelli and G. Parisi, Nucl. Phys. B126 (1977) 298.

[35] M. G. Ryskin, Z. Phys. C37 (1993) 89.

[36] L. Frankfurt, invited talk at the Minischool on Diffractive Physics, DESY, May 1994.

[37] L. L. Frankfurt and M. Strikman, Phys. Rev. Lett. 64 (1989) 1914.

[38] A. H. Mueller and W. K. Tang, Phys. Lett. B284 (1992) 123

[39] J. R. Forshaw and M. G. Ryskin, hep-ph/950376.

[40] V. L. Chernyak and A. R. Zhitnitski, Phys. Rep. 112 (1984) 173.

[41] Review of Particle Properties, Phys. Rev. D50 (1994) 1177.

[42] L. L. Frankfurt and M. Strikman, Nucl. Phys. B250 (1985) 147.

[43] S. Brodsky and A. H. Mueller, Phys. Lett. 206B (1988) 685.

[44] L. L. Frankfurt, M. Strikman and S. Liuti, Phys. Rev. Lett. 65 (1990) 1725.

[45] B. K. Kopeliovich, J. Nemchik, N. N. Nikolaev and B. G. Zakharov, Phys. Lett. B324 (1994) 469; B. K. Kopeliovich and B. G. Zakharov P(TH)-1993-27.

[46] L. L. Frankfurt, M. Sargsyan and M. Strikman, in preparation.

[47] V. Franco and R. G. Glauber, Phys. Rev. 142 (1966) 1195.

[48] M. R. Adams et al., FERMILAB-PUB-94-233-E, 1994.

[49] J. C. Collins, L. L. Frankfurt and M. Strikman, Phys. Lett B307 (1993) 161.

[50] L. L. Frankfurt, " Hard diffractive processes at colliders", talk at the FAD meeting at Dallas, TX, March 1992.

[51] A. Berera and D. Soper, Phys. Rev. D50 (1994) 4328.

[52] G. Ingelman and P. Schlein, Phys. Lett. B152 (1985) 256.

[53] UA8 Collaboration, A. Brandt et al., Phys. Lett. B297 (1992) 417.

[54] A. Donnachie and P. V. Landshoff, Phys. Lett. B285 (1992) 172.

[55] M. Diehl, DAMTP-94-60 (1994).

[56] M. Ryskin and M. Besancon, in Proceedings of the HERA Workshop, "Physics at HERA", vol.1, edited by W. Buchmuller and G. Ingelman, (1991) 215.

[57] J. Bartels, H. Lotter, M. Wusthoff, DESY preprint 94-245 (1994).

[58] E. A. Kuraev, L. N. Lipatov and V. S. Fadin, Sov. Phys. JETP 44 (1976) 443; Sov. Phys. JETP 45 (1977) 199. Y. Y. Balitsky and L. Lipatov, Sov. J. Nucl. Phys 28 (1978) 822.

[59] L. V. Gribov, E. M. Levin, M. G. Ryskin, Phys. Rep. 100 (1983) 1.

[60] A. H. Mueller and J. Qiu, Nucl. Phys. B268 (1986) 427

[61] M. G. Ryskin, Yad. Fiz. 50 (1989) 1428.

[62] B. Badelek, M. Krawczyk, K. Charchula, J.Kwiecinski, Rev. Mod. Phys. 64 (1992) 927.

[63] H. L. Lai, J. Botts, J. Huston, J. G. Morfin, J.F. Owens, J. Qiu, W. K. Tung and H. Weerts, Preprint MSU-HEP/41024, CTEQ 404.

[64] E. Laenen and E. Levin, Ann. Rev. Nucl. Part. Sci. 44 (1994) 199.

[65] A. J. Askew, J. Kwiecinski, A. D. Martin, P. J. Sutton, Phys. Rev. D49 (1994) 4440

[66] J. Collins and J. Kwiecinski, Nucl. Phys. B335 (1990) 89.

[67] J. D. Bjorken, summary talk in Proceedings of the Colloqium on High Multiplicity Hadronic Interactions, Paris, May 1994., ed. A. Krzywicki (Ecole Polytechnique).

[68] H. Cheng and T. T. Wu, " Expanding Protons: Scattering at High Energies", The MIT Press, Cambridge, Massachusetts, London, England.

[69] L. D. Landau and E. M. Lifshitz, "Quantum mechanics".

[70] V. N. Gribov, Sov. Phys. JETP 30 (1969) 709.

[71] J. D. Bjorken in Proceedings of the International Symposium on Electron and Photon Interactions at High Energies, p. 281–297, Cornell (1971).

[72] E. M. Levin, M. Wusthoff, Phys. Rev. D50 (1994) 4306.

[73] J. D. Bjorken and J. B. Kogut, Phys. Rev. D8 (1973) 1341.

[74] ZEUS Collaboration, M. Derrick et al., Z. Phys. C63 (1994) 391.

[75] R. P. Feynman, " Photon-hadron interactions", W. A. Benjamin, Inc, Reading, Massachusetts, 1972.

[76] Yu. Dokshitzer, invited talk at the Minischool on Diffractive Physics, DESY, May 1994.

[77] B. Blättel, G. Baym, L. L. Frankfurt, H. Heiselberg and M. Strikman, Phys. Rev. D47 (1993) 2761.

[78] G. A. Schuler and T. Sjöstrand, Nucl. Phys. B407 (1993) 539; "Total Cross–Sections for Reactions of High Energy Particles", Lndolt–Börnstein, New Series, Vol. 12b, H. Shopper, ed. (1987).

[79] S. Abachi et al., Phys. Rev. Lett. 72 (1994) 965.